AD-A237 683

NAVAL POSTGRADUATE SCHOOL
Monterey , California

DTIC
ELECTE
JUL 01 1991
C

THESIS

AN INVESTIGATION OF THE ERICA IOP-2

CYCLONE USING THE NORAPS MODEL

by

Ronald J. Miller

June 1990

Thesis Advisor   Carlyle H. Wash

Approved for public release; distribution is unlimited.

91-03253

91 C 2 0 0

REPORT DOCUMENTATION PAGE

Form Approved
OMB No 0704-0188

1a REPORT SECURITY CLASSIFICATION Unclassified	1b RESTRICTIVE MARKINGS
2a SECURITY CLASSIFICATION AUTHORITY	3 DISTRIBUTION/AVAILABILITY OF REPORT Approved for public release; distribution is unlimited.
2b DECLASSIFICATION/DOWNGRADING SCHEDULE	
4 PERFORMING ORGANIZATION REPORT NUMBER(S)	5 MONITORING ORGANIZATION REPORT NUMBER(S)

6a NAME OF PERFORMING ORGANIZATION Naval Postgraduate School	6b OFFICE SYMBOL (If applicable) 63	7a NAME OF MONITORING ORGANIZATION Naval Postgraduate School
6c ADDRESS (City. State, and ZIP Code) Monterey, CA 93943-5000		7b ADDRESS (City, State, and ZIP Code) Monterey, CA 93943-5000

8a NAME OF FUNDING SPONSORING ORGANIZATION	8b OFFICE SYMBOL (If applicable)	9 PROCUREMENT INSTRUMENT IDENTIFICATION NUMBER

8c ADDRESS (City, State, and ZIP Code)	10 SOURCE OF FUNDING NUMBERS			
	PROGRAM ELEMENT NO	PROJECT NO	TASK NO	WORK UNIT ACCESSION NO

11 TITLE (Include Security Classification)

An Investigation of the ERICA IOP-2 Cyclone Using the NORAPS Model

12 PERSONAL AUTHOR(S)
Ronald J. Miller

13a TYPE OF REPORT Master's Thesis	13b TIME COVERED FROM _____ TO _____	14 DATE OF REPORT (Year, Month, Day) June 1990	15 PAGE COUNT 88

16 SUPPLEMENTARY NOTATION The views expressed in this thesis are those of the author and do not reflect the official policy or position of the Department of Defense or U.S. government.

17	COSATI CODES		18 SUBJECT TERMS (Continue on reverse if necessary and identify by block number)
FIELD	GROUP	SUB-GROUP	Rapid cyclogenesis, ERICA, NORAPS

19 ABSTRACT (Continue on reverse if necessary and identify by block number)
Rapid cyclogenesis is studied using the U.S. Navy Operational Regional Atmospheric Prediction System (NORAPS) numerical model. The cyclone studied occurred during the second Intensive Observation Period (IOP-2) of the Experiment on Rapidly Intensifying Cyclones over the Atlantic (ERICA). Several simulations were run to examine the inability of this and other operational numerical models to correctly predict development, movement, and other characteristics of this cyclone. The experiments consisted of varying the cumulus parameterization and the initial low-level temperature and moisture fields. The exact cumulus specification did not appear to have a significant effect on the forecast sea level pressure. Although convective precipitation amounts varied with different parameterizations, the stable precipitation recovered the difference resulting in a nearly equivalent amount of latent heating. A dry simulation showed that the latent heat released from precipitation is necessary to achieve the observed deepening rate. A poor analysis over the data-sparse ocean and lack of a moisture

20 DISTRIBUTION AVAILABILITY OF ABSTRACT ☒ UNCLASSIFIED/UNLIMITED ☐ SAME AS RPT ☐ DTIC USERS	21 ABSTRACT SECURITY CLASSIFICATION Unclassified	
22a NAME OF RESPONSIBLE INDIVIDUAL Carlyle H. Wash	22b TELEPHONE (Include Area Code) (408) 646-2295	22c OFFICE SYMBOL 63Wx

DD Form 1473, JUN 86 Previous editions are obsolete   SECURITY CLASSIFICATION OF THIS PAGE

S/N 0102-LF-014-6603

19. ABSTRACT (continued)

analysis caused the modeled atmosphere to be too potentially unstable, resulting in much more precipitation and development than was observed early in the forecast period. A simulation using the global analysis fields for initialization, which were somewhat cooler and drier than the NORAPS initial fields, resulted in a better forecast, although the observed deepening rate was not achieved. All simulations incorrectly develop the first of two lows. Numerical models run at the National Meteorological Center (NMC) also failed to correctly deepen the secondary low, and varied greatly in their predicted deepening rates.

An Investigation of the ERICA IOP-2
Cyclone using the NORAPS Model

by

Ronald J. Miller

Research Meteorologist,
Naval Oceanographic & Atmospheric Research Laboratory,
Atmospheric Directorate
B. S., San Jose State University, 1985

Submitted in partial fulfillment of the
requirements for the degree of

MASTER OF SCIENCE IN METEOROLOGY

from the

NAVAL POSTGRADUATE SCHOOL
June 1990

Author: _____
           Ronald J. Miller

Approved by: _____
           Carlyle H. Wash, Thesis Advisor

_____
           Wendell L. Nuss, Second Reader

_____
           Robert J. Renard, Chairman,
           Department of Meteorology

iii

TABLE OF CONTENTS

ACKNOWLEDGEMENTS

I. INTRODUCTION

During the past few decades, weather forecasting accuracy has increased largely due to the improvements in numerical modeling of the atmosphere. Forecasts of 1 - 3 days can be made with a good deal of certainty, allowing for necessary preparations to be made for oceanic or continental winter storms. However, rapidly changing events such as explosive cyclogenesis are still often missed by the numerical models and the human forecaster. This remains a potentially hazardous situation since people are often caught unprepared with little or no warning.

While the fundamentals of cyclogenesis are generally understood and documented, the factors which combine to create a rapidly deepening cyclone are still unclear. Operational forecast models used for 1 to 3 day forecasts have consistently tended to under-forecast the deepening rate of these storms (Sanders and Gyakum 1980), although more recent studies have shown an improvement in this area (Sanders 1987). A number of reasons have been suggested to account for this failure including spatial resolution, initial conditions, and subgrid-scale parameterizations.

A large number of studies using numerical model simulations of explosive cyclogenesis have been conducted. In general, these studies fall into two categories. The first group includes near perfect model simulations allowing for diagnostic studies. These studies allow researchers to get a more complete and dynamically consistent picture of the developing cyclone, even though actual data measurements are sparse temporally and spatially (e.g., Whitaker et al. 1988; Uccellini et al. 1987). The second kind of study involves investigations of model failures to match the observed deepening rate of an extratropical cyclone (e.g., Anthes et al. 1983). As numerical models usually under-predict the observed deepening rate, various parameterizations and resolutions are varied in an attempt

1

to improve the model forecast, with varying degrees of success. This thesis, however, will investigate a failure of a numerical model which forecast overdevelopment of an explosively deepening extratropical cyclone.

Recently, large scale experiments have been conducted in order to study the explosive deepening of extratropical cyclones. The most recent of these was the Experiment on Rapidly Intensifying Cyclones over the Atlantic (ERICA), conducted from 1 December 1988 to 1 March 1989 (Hadlock 1988; Hartnett et al. 1989). Its purpose was to provide a large data sampling of such cyclones over the open waters of the western North Atlantic Ocean. Aircraft, buoys, increased rawinsondes, and radar data supplemented the usual satellite imagery during Intense Observation Periods (IOP's).

The second storm of the experiment, IOP-2, developed on 13-14 December 1988. The Naval Operational Regional Atmospheric Prediction System (NORAPS) forecast initialized at 12Z on 12 Dec 88 missed the time and rate of rapid deepening of the IOP-2 cyclone, although its 48 h forecast of central pressure was only 6 mb off. Using additional buoy and dropsonde data obtained during ERICA, this study will investigate the successful and unsuccessful aspects of the model's forecasts.

A literature review is presented in section 2 focusing on the latent heating aspect of rapid cyclogenesis. Section 3 summarizes the synoptic events of IOP-2 and briefly describes the operational numerical forecasts of this cyclone. A brief description of the NORAPS model is given in section 4. The numerical simulations made using the NORAPS model are documented in section 5, followed by a diagnostic study of these simulations in section 6.

II. BACKGROUND

Numerous studies have been conducted to investigate the causes of explosive cyclogenesis and the reasons for poor forecasts of these events by numerical models. Anthes et al. (1983) described model simulations of the QE II storm. Their study concluded that lower tropospheric baroclinic instability was the major cause of growth for that cyclone. This result was confirmed by composite rawinsonde data studies from weather ships (Rogers and Bosart 1986). However, Uccellini (1986) has shown that upper-tropospheric conditions were also important in the QE II storm.

Anthes et al. (1983) state that latent heat release appeared to be more important in the latter stages of development. Numerical simulations with and without latent heating showed little difference in the 12 h forecast, indicating the lack of importance in latent heating for the early period of development of that case. While the increased latent heating improved the intensity forecast, the predicted motion of the storm was slowed due to this heating, resulting in larger position errors. Recent studies also have shown that the vertical distribution of latent heating has a significant effect on the deepening the storm, with a lower height of maximum heating producing a greater intensification. Danard (1985) postulates that this is due to a lower level of non-divergence and increased low level convergence and vorticity production. The heating of the lower troposphere also causes destabilization, resulting in a more rapid intensification.

Danard (1985) studied two explosive deepening events in the eastern North Pacific using an 8-level large scale (190 km grid spacing) primitive equation model. He too concluded that both latent and sensible heating play a major role in cyclone intensification. Three variations of the cumulus parameterization scheme developed by Kuo (1974)

3

indicated that the underlined maximum amount of underlined convective precipitation was directly proportional to the amount of deepening, although the differences were not large (5 mb at most).

Leslie et al. (1987) conducted model simulations of an explosively deepening cyclone off the east coast of Australia. Their findings on the role of precipitation agreed with Anthes et al. (1983). For their case study it appears that cumulus convection is not important during the early stages of the cyclone formation, but plays a decisive role in the rapid intensification stage. They also tested the importance of other small scale processes such as effects of topography, surface fluxes, and sea-surface temperature analyses. They concluded that all effects were necessary for cyclone development and that none could be omitted without degrading the forecast significantly. Even with 25 km horizontal resolution, they failed to achieve the observed deepening rate.

Mullen and Baumhefner (1988) pointed out that case studies of individual storms can be misleading and that the results cannot always be generalized. Their study used an 11 western North Pacific Ocean storm ensemble from the NCAR Community Climate Model. From a 150-day simulation of perpetual January conditions, their results indicate that total diabatic heating and baroclinic dynamics contribute equally to storm development. Additionally, sensible and latent heating are each responsible for approximately one-half of the deepening due to diabatic processes. They also found that the deepening rate was insensitive to the exact specification of precipitation parameterization although they cautioned not to rule out other schemes.

Robertson and Smith (1983) conducted a diagnostic energetics analysis of extratropical cyclone development using the Limited Area Mesoscale Prediction System (LAMPS) from Drexel University. Two versions of the model, moist and dry, were run on two case studies. Their results also show that the baroclinic aspects of development are greatly enhanced by both convective and stable latent heat release in the model. In the moist

4

forecasts, a substantial amount of eddy kinetic energy is generated due to ageostrophic flow induced by diabatic heating.

A comprehensive study on numerical prediction of explosive cyclogenesis was recently conducted by Kuo and Low-Nam (1990) They ran 24 h simulations of 9 nine explosive cyclones over the western Atlantic ocean, varying the grid resolution, cumulus parameterization, initial and boundary conditions, as well as surface fluxes. Their results indicate that the most crucial model component for short range (0-24 h) prediction of rapid cyclogenesis is the initial conditions, followed by the horizontal grid resolution, precipitation parameterization, and lateral boundary conditions, with surface fluxes playing a minor role. More interesting is their finding that upright convection actually degraded the forecast due to an incorrect location of heating. Grid scale precipitation (i.e., non-convective or stable) associated with the slantwise ascent in the warm front was crucial for rapid development. Simulations using the Arakawa-Schubert (1974) scheme produced superior forecasts to those using Kuo (1974). But this was thought to be caused by the fact that the Arakawa-Schubert scheme resulted in much lower convective precipitation amounts, thus allowing more of the available moisture to be used by the stable precipitation scheme. They also concluded that the Kuo scheme was too easy to activate.

Most recently, two studies were conducted on cyclones from the Genesis of Atlantic Lows Experiment (GALE) using the NORAPS model. Liou et al. (1990) ran the model on the Intensive Observation Period (IOP) 2 cyclone with and without the extra data obtained as a result of experiment. Since the cyclogenesis and development were along the east coast of the U.S., the additional data from the experiment resulted in only a limited improvement on the NORAPS analyses and forecasts (e.g., 1 - 3 mb in central pressure). In general, NORAPS predicted the cyclogenesis event fairly well in the short term (24 - 36 h) but missed the strength and timing of a cold surge resulting in poor forecasts later in the period. Secondary cyclogenesis at 36 h was correctly forecast by the model. Wash et al.

(1990) studied the GALE IOP9 cyclone. Using the additional GALE observations, the NORAPS optimal interpolation analysis reveals critical subsynoptic features which were important in the development. However, NORAPS incorrectly deepened the wrong low due to a poorly forecast 250 mb jet streak. Central pressures were under-forecast by 10-15 mb after 36 h. NORAPS forecasts using the additional GALE data were better on the storm track but still deficient on intensity.

The current study also investigates the importance of latent heating in the development of an explosively deepening cyclone. However, the regional model used in this study operationally over-predicted the deepening of the ERICA IOP-2 cyclone. The importance of the model initial conditions also will be studied. ERICA data (aircraft dropsondes, rawinsondes, and buoys) will be used to verify the model performance. The results should yield a better understanding of numerical modeling processes in forecasts of explosive cyclone development.

III. ERICA IOP-2 SYNOPTIC SUMMARY

During the development of the ERICA IOP-2 cyclone, two disturbances of different origins interacted over the western North Atlantic Ocean to produce a rapidly deepening surface low (Chalfant 1989). Figure 1 presents the Fleet Numerical Oceanography Center's (FNOC) 500 mb analysis for 1200 UTC 12 December 1988[1]. A large trough lies over eastern Canada and extends along the east coast of the United States. East of the Virginia coastline, two air streams merge, one originating from Northwest Canada, the other from the southeastern U.S.

By 13/0000, short wave troughs are apparent in each of the air streams (Fig. 2). The northerly wave is located over Michigan and Wisconsin with the southerly disturbance over the southeast U.S. Note the phase lag of the -30°C isotherm compared to the height and wind field in the northern trough (over Minnesota), indicating the likelihood of additional baroclinic development. The FNOC surface analysis for this time (Fig. 3) reveals a cold front extending southwestward from a low near 40°N 50°W to the southern tip of Florida. Behind it, a high pressure system is moving off the New England coastline. The winds associated with the high are advecting cold air over the warm Gulf Stream waters. Note that buoy 41001 at 35°N 73°W is reporting an air temperature of 10°C and a sea-surface of 20.5°C.

A surface low begins to develop along the tail end of the cold front off the Florida coast after 13/0000 in response to the southerly short wave. The low slowly deepens and moves northeastward over the next 12 h as seen in Fig. 4. Meanwhile at 500 mb, the northerly trough has continued to develop and move to the Ohio Valley (Fig. 5). Note,

---

1. Hereafter, date and time will be denoted in a day/hour UTC format, e.g. 12/1200.

7

however, that this upper-level wave is not associated with any well defined surface low, although a surface trough does extend from the Great Lakes to Kentucky with some reports of snow (Fig. 4). By 13/1800 (not shown), a second surface low has formed east of Cape Hatteras in response to the northerly trough.

The operational objective surface analyses without ERICA data do not accurately depict this developing cyclone situation. Thus, subjective analyses by Chalfant (1989), utilizing satellite imagery and ERICA aircraft and buoy data, are used. At 14/0000 (Fig. 6), three lows appear with central pressures between 996 and 998 mb. Aloft (Fig. 7), the northern wave has moved off the East Coast of the US. Note that the isotherms are now more nearly in phase with the height contours, indicating little or no further baroclinic development aloft is expected. However, at the surface, the rapid intensification event begins at this time.

The surface analysis at 14/0600 (not shown) shows the lows have merged and deepened approximately 17 mb over 6 h. By 14/1200 (Fig. 8), the low has plummeted to at least 968 mb (buoy at 37.5°N 63.5°W), a drop of 30 mb in 12 h. As was expected from the 14/0000 500 mb analysis of heights and temperatures (Fig. 7), the height of the upper-level short wave (5340 m over Delaware) has shown little change over the same 12 h period (Fig. 9), although a closed circulation has developed.

Operational numerical forecasts of the IOP-2 cyclone varied in accuracy. They are evaluated in detail by Chalfant (1989). None could successfully resolve the multiple low centers at 14/0000. The NMC's Nested Grid Model (NGM) 48 h surface pressure forecast valid at 14/1200 (not shown) indicates only a 984 mb low, an error of 16 mb. However, the position forecast is only 100 km in error. The Global Spectral Model, also run at NMC, produced a much better forecast with central pressure of 964 mb (not shown) and a position error equivalent with the NGM. The operational NORAPS forecast (Simulation 1 in section 5) correctly predicted the rapid deepening, showing a 962 mb low at 48 h, but a

8

position error of approximately 350 km. However, as will be shown, the impressive fore-cast of rapid deepening at 48 h by NORAPS and the NMC spectral model is actually the result of poor forecasts at intermediate times.

IV. MODEL DESCRIPTION

NORAPS is a regional model run operationally by FNOC, Monterey, CA over four areas: the Mediterranean Sea, the Indian Ocean, the North Atlantic Ocean, and the western North Pacific Ocean. The purpose of NORAPS is to provide high resolution forecasts of up to 48 h for areas important to Navy operations (Hodur 1987). The NORAPS model is easily relocatable to any area of the globe. The grid spacing is variable, both horizontally and vertical, but is limited by the speed and memory constraints of the computer system. For simulations in the current study, 60 km spacing is used on a 109 x 82 grid providing a model domain of approximately 6480 x 4860 km (Fig. 10). The vertical distribution of the 21 vertical sigma levels is shown in Table 1.

Table 1. NORAPS model sigma levels

Model Level	Sigma	Model Level	Sigma
1	0.010	12	0.600
2	0.035	13	0.700
3	0.067	14	0.787
4	0.105	15	0.850
5	0.150	16	0.890
6	0.200	17	0.920
7	0.250	18	0.950
8	0.300	19	0.975
9	0.350	20	0.990
10	0.412	21	0.997
11	0.500		

NORAPS obtains initial data from radiosonde, PIBAL, aircraft and ship observations. In certain regions, satellite vertical soundings and cloud-track winds are used. Optimum Interpolation (OI) is used for the analysis of these data with the previous 12 h forecast used as the first guess field. In order to "spin up" the model, four 12 h update cycles are run

before a realistic simulation is performed. To begin the update cycle, the NOGAPS (Naval Operational Global Atmospheric Prediction System) analyses are used as first guess fields. Neither NORAPS nor the global model NOGAPS perform a moisture analysis. Thus, the previous 12 h moisture forecast is used as the analysis.

Boundary conditions for the forecast fields in the NORAPS model run are obtained from NOGAPS forecasts. NORAPS uses one-way interactive lateral boundary conditions, which create a "blend zone" near the edge of the model grid. If the global model provides a poor representation of conditions on the NORAPS boundary, the forecast in the interior of the domain will eventually be contaminated. The length of time it takes for contamination to occur depends largely on the speed at which the wind field advects the boundary conditions across the domain. The longer the forecast, or the smaller the model domain, the more likely it is that poor boundary conditions may adversely affect the NORAPS forecast. For the present study, the model domain was situated so that its left boundary was far upstream of the incipient cyclone in order to minimize the effects of the boundary conditions (Fig. 10).

Topography in NORAPS is obtained from the Navy ten minute global data base. A terrain enveloping procedure developed by Wallace et al. (1983) is used to more effectively represent terrain effects in the model. A land-sea table with ten minute resolution is used by the model to define land and sea grid points. Over water, the albedo is set to 0.09, the ground wetness is 1.0, and the surface roughness is computed. Over ice, these values are 0.6, 0.0, and 0.0002435 m, respectively. Monthly climatological values are used for the land grid points, as well as the sea-surface temperature.

The model uses an Arakawa Type-C staggered grid (Arakawa and Lamb 1977). Time integration is performed using a split-explicit scheme developed by Madala (1982). In this method, the solution is adjusted for the linear terms which govern the fastest gravity modes, permitting use of a relatively large model time step. All advection terms are

11

second order. Fourth-order diffusion is included in the interior with second order diffusion on the first row and column of the grid. High frequency time oscillations are controlled by applying a Robert (1966) time filter with the smoothing coefficient set to 0.15.

The parameterization of surface fluxes in the planetary boundary layer (PBL) are computed using the similarity theory (Louis et al. 1982), where matching solutions are obtained for the constant flux layer and the Ekman layer. The scheme is first order K-theory where K is a function of the bulk Richardson number.

Since the lowest model sigma level above the surface is equal to 0.9975, a predictive equation for ground temperature given by Blackadar (1977) is used for land grid points. The radiation parameterization follows the methods of Sasamori (1968) for long wave radiation and Arakawa (1971) for short wave radiation. The effects of clouds are incorporated into both radiation parameterizations, while short wave radiation includes a diurnal cycle.

Precipitation in NORAPS can occur from convective processes (sub-grid scale) or from large-scale condensation. Convection is parameterized using a Kuo-type scheme (Kuo 1965; Kuo 1974), in which precipitation is linked to low-level moisture convergence. With each time step, the model determines whether a grid point meets the necessary conditions for convection. First, there must be moisture convergence in the PBL. Mathematically,

$$M_t = (P_s/g) \int \nabla \cdot q\mathbf{V} \, dp > 0$$

where M_t is the moisture convergence, P_s is the surface pressure, g is gravity, q is the specific humidity, and the integral is performed over a depth of the atmosphere.

Secondly, the value of Θ_e above the LCL must be less than that at the LCL (i.e., a conditionally unstable layer must exist above the LCL). The depth of this conditional

instability must be greater than 300 mb. Finally, the relative humidity at the originating level must be greater than 80%.

If the four conditions are met, the model transports heat and moisture vertically to each level (subscript k) using the equations given by Kuo (1965),

$$
\delta T_k \;=\; \frac{M_t \,(T_c - T)_k}{\frac{1}{g}\int C_p \,(T_c - T)\,dp \;+\; \frac{1}{g}\int L\,(q_c - q)\,dp}
$$

$$
\delta q_k \;=\; \frac{M_t \,(q_c - q)_k}{\frac{1}{g}\int C_p \,(T_c - T)\,dp \;+\; \frac{1}{g}\int L\,(q_c - q)\,dp} \;.
$$

Here, T and q are temperature and specific humidity respectively, where the c subscript denotes cloud and unsubscripted denotes the environment. C_p represents specific heat and L is latent heat. Integrations are performed over the depth of the cloud (i.e., where $(T_c - T)$ > 0).

Kuo (1974) modified his parameterization with the inclusion of the "b" factor. This regulated the amount of heating verses moistening that occurs in the scheme. The fraction "b" is calculated following

$$
b \;=\; \frac{100\% - R}{100\% - 50\%} \;,
$$

where R equals the integrated relative humidity over the depth of the cloud and 100% > R > 50%. Now the equations are modified as follows:

$$
\delta T_k \;=\; \frac{(1 - b)\,M_t \,(T_c - T)_k}{\frac{1}{g}\int C_p \,(T_c - T)\,dp}
$$

$$
\delta q_k \;=\; \frac{b\,M_t \,(q_c - q)_k}{\frac{1}{g}\int L\,(q_c - q)\,dp} \;.
$$

The role of "b" is to allow for rapid moistening initially when R is small (large b). As the column moistens, R increases and b decreases. This enhances the latent heating and decreases the moistening rate.

At the time of IOP-2 (December, 1988), the NORAPS model operationally used the Kuo (1965) scheme. In April of 1989, the Kuo (1974) scheme was incorporated. Thus, the simulations in section 5 reproduce the operational forecast of December, 1988, as well as the current operational version.

Stable (or nonconvective) precipitation is assumed to occur when a grid point becomes supersaturated. Moisture is condensed until saturation is once again reached. The condensed moisture is evaporated into the next layer below until it becomes saturated.

The NORAPS model has been used operationally by the U.S. Navy since 1984. Skill scores show its forecast accuracy to be comparable with other numerical models (Hodur 1987). In addition, the NORAPS model has been used extensively as a research tool at the Naval Oceanographic and Atmospheric Research Laboratory and the Naval Postgraduate School. Recent studies (Liou et al. 1990; Wash et al. 1990) have utilized the model to study cyclogenesis during GALE.

V. MODEL SIMULATIONS

In order to investigate the physical processes of this rapidly deepening cyclone, numerical simulations of the cyclone were run using the NORAPS model. Forecasts of 48 h were made beginning at 12/1200, 12 h before the initial development and 36 h before the rapid deepening. Since the intensification occurred with significant convection (Chalfant 1989), the convective parameterization scheme of NORAPS was varied with all other physics in the model treated identically. The four convective parameterization schemes that were run are: 1) Kuo (1965) cumulus scheme (which was the operational version in December, 1988); 2) Kuo (1974); 3) Kuo (1974) with vertical eddy diffusion; 4) convective and stable precipitation turned off[2].

A. SIMULATION 1

Simulation 1 of the IOP-2 event appears to begin well. A weak low forms at 30°N off the Florida coast by 13/0000 (Fig. 11). But comparison with Fig. 3 shows that the forecast low is northeast of the verifying position by over 750 km. This is a large error for a 12 h forecast.

Figures 12 and 13 present the (a) 1000 mb streamlines and (b) 500 mb heights and vorticity for the analysis (12/1200) and 12 h forecast (13/0000) respectively. A weak 500 mb disturbance is located over Florida in the analysis as indicated by the 8 s^{-1} vorticity contour (Fig. 12b). An examination of actual rawinsonde data (not shown) indicates that the disturbance did exist as a result of cyclonic shear across northern Florida. As this disturbance moves off the coast, it becomes superimposed over the trailing cold front, as

---

2. Hereafter, the Kuo (1965) and Kuo (1974) schemes will be denoted KUO65 and KUO74 respectively.

shown by the surface streamlines (Fig. 12a). This system develops rapidly during the 12 h period as the 500 mb absolute vorticity doubles from $8\ s^{-1}$ to $16\ s^{-1}$ (Fig. 13b). However, there has been no corresponding change in the height contours to account for such a change in vorticity.

Note that the southerly short wave mentioned in section 4 is still over the southeastern U.S., as indicated by the vorticity maxima over Georgia in Fig. 13b. There is very little indication of the existence of this weak shortwave over Florida in the actual 500 mb analysis for 13/0000 (Fig. 2), although by 13/1200 (Fig. 5) it appears near 30°N 65°W, but apparently no surface development took place. In other words, NORAPS incorrectly developed a surface low well to the east of the southerly wave in the IOP-2 event. The existence of this low at the surface is not verified by observational data, although the weak 500 mb wave did, in fact, exist. Comparing Figs. 13a and 13b, it is noted that the forecast 1000 mb circulation is southwest of the vorticity maxima at 500 mb. Thus, the low is actually lying under negative vorticity advection. Closer inspection reveals that the low-level convergence zone northeast of the 1000 mb low is directly under the 500 mb vorticity maxima.

Figure 14 shows the 12 h cumulative convective precipitation forecast by the model. Note that the precipitation maxima lies directly over the 1000 mb convergence zone northeast of the low (Fig. 13a). This is not surprising, since low-level moisture convergence is one of the four necessary conditions for convection in the Kuo scheme (see Section 3). The convective precipitation is also coincident with the 500 mb vorticity maxima (Fig. 13b). While some surface observations do indicate some shower activity in this area, there is nothing to substantiate the predicted 2.8 cm of convective rainfall. Thus, the first 12 h of the model simulation can be summarized as follows: a weak upper-level short wave trough moved over a low-level baroclinic zone east of Florida, initiating cyclogenesis. Low-level convergence associated with the surface low triggered convection northeast of

16

the incipient cyclone. The model convection produces an erroneous vorticity maxima at 500 mb.

This is even more apparent in Fig. 15 where the 18 h 500 mb heights and vorticity, and the 12 to 18 h convective precipitation fields are compared. The model continues to successfully predict the real short wave over the Georgia coastline (Fig. 15a). But it is obvious that the height and vorticity pattern to the east is anomalous. The model predicts 12.1 cm of convective rainfall to occur at a grid point during the past 6 h with a secondary maxima of approximately 7 cm to the east. Comparing this to Fig. 15a, note the collocation of the 12.1 cm rainfall maxima and the small ridging in the 5640 m line at 500 mb likely due to the diabatic heating. Once again, the convective precipitation lies over the convergent region north and east of the 1000 mb low (not shown).

As the upstream short wave in Fig. 15a merges with the developing system, rapid deepening takes place (7 mb in 6 h, 17 mb in 12 h, and 28 mb in 18 h). By 14/0000, the model has deepened the low to 980 mb (Fig. 16). A comparison with the subjective analysis in Fig. 6 shows the failure of the model forecast. Only one low is predicted which is 16-18 mb too deep and too far north, although a surface trough northwest of the low does hint at a secondary development as does the convective precipitation (not shown). The 500 mb forecast (not shown) still contains the intense northerly short wave trough moving off the east coast of the US. However, the initial low has already developed too much to allow the new short wave to create a new low.

Finally, Fig. 17 shows the 48 h NORAPS forecast at the surface and 500 mb. The forecast surface low is only a few millibars too deep (assuming the 968 mb buoy is a true representation of the central pressure), but the position error is approximately 500 km (Fig. 8). At 500 mb, the low is similarly too deep and too far north.

In summary, it appears that the operational NORAPS model predicted both 500 mb synoptic features reasonably well: the southerly short wave from Florida, and the norther-

ly wave from Canada. Unfortunately, the model over-forecast the development of a weak low which preceded the southerly short wave. By the time the northerly short wave arrived, the initial low was too well developed to permit secondary development. Instead, the northerly wave could only contribute to the deepening of the existing low.

Several studies have shown that enhanced precipitation occurs in an area extending from the northeast to the north and west of a surface low prior to the onset of rapid deepening (Krishnamurti 1968; Johnson and Downey 1976; Kocin and Uccellini 1989). Kuo and Low-Nam (1990) found that this warm frontal precipitation was crucial to the explosive development of the cyclone. The warm front predicted by the model, as seen in the 1000 mb wind field and the convective precipitation pattern, is in agreement with these findings.

Examination of the model output reveals that during the development of the surface low, the low is located either directly under the 500 mb vorticity maxima or upstream of it. One would expect the low to be located downstream of the vorticity maxima in the region of the positive vorticity advection. In addition, convective precipitation charts indicate that the convective nature of this storm contributed heavily to its development. While ship reports and satellite imagery verify that convective activity was present (not shown), it is unlikely that the model simulation is accurate in this respect. To investigate the convective aspect of the model simulation, diagnostics of the effects of convection are presented in the next section.

B. SIMULATION 2

A known deficiency of the KUO65 scheme is that it added too much moisture aloft (Kuo 1974). In order to correct for this, the "b" factor was added which reduces the moistening when near saturation is reached (see discussion of convection parameterization in section 3). Simulation 2 used the KUO74 scheme to see if the change made any difference in the IOP-2 case.

Figure 18 presents the 6 h cumulative convective precipitation predicted by the model valid at 13/0600. Comparing this with Fig. 15b, it is apparent that the KUO74 scheme has reduced the convective rainfall amount by more than 50%. However, the surface and 500 mb forecasts (not shown) at all times were nearly identical to that of Simulation 1 (1 - 2 mb differences in the central sea level pressure). The reason for the nearly identical forecast is that the stable precipitation was greater in Simulation 2, as shown by Table 2. In other words, since the KUO74 scheme caused less <u>convective</u> precipitation, there was more moisture available for the <u>non-convective</u> scheme. As Table 2 indicates, the <u>total</u> amount of precipitation in Simulation 2 is nearly equal that of Simulation 1. Therefore, the amount of latent heat released in the two simulations is nearly equal, resulting in comparable forecasts. Danard (1985) and Liou and Elsberry (1987) observed a direct correlation between the maximum amount of convective precipitation and the predicted deepening rate. Kuo and Low-Nam (1990) found that the amount of stable precipitation was key to determining the amount of deepening. In the current study the total precipitation was correlated to the deepening rate.

Table 2. Precipitation (cm) predicted by the NORAPS model for Simulations 1, 2, 3, and 5. The amounts are a 48 h sum of all grid points with precipitation caused by the IOP-2 cyclones. Also included is the predicted central pressure (mb) at 48 h.

	Simulation			
	1	2	3	5
Convective	1929	1625	1547	1470
Stable	578	826	859	575
Total	2507	2451	2406	2045
Cent. Press.	962	960	962	971

C. SIMULATION 3

The inclusion of vertical eddy diffusion in the convection scheme was tested in Simulation 3. The effect of this diffusion is to mix the heat and moisture provided by the cumulus parameterization with the surrounding environment. This addition was expected to damp the effects of convection predicted by the model. As seen in Table 2, the convective precipitation was further reduced by the eddy diffusion. However, once again the stable precipitation was greater as a result. Thus, Simulation 3 showed little difference from the previous two simulations.

D. SIMULATION 4

A fourth simulation was conducted in which no precipitation was allowed. The goal of this simulation was to ensure that the convective precipitation scheme was truly responsible for the poor forecasts observed in the first three simulations. It was unrealistic since no convective or stable precipitation was allowed. In other words, when a grid point became super-saturated, the model did nothing to correct this condition. Any development that takes place is due only to adiabatic baroclinic dynamics, since there is no latent heat release.

Figure 19 shows the (a) 1000 mb winds and (b) 500 mb heights and vorticity for the 12 h forecast. There are marked differences between this simulation and Simulation 1 (Fig. 13). The initial short wave at 500 mb over Florida does not develop in Simulation 4 (note that the enclosed area of 8 s^{-1} vorticity near 70 W in Fig. 19b is a minimum). Moreover, no development from this system takes place at 1000 mb (Fig. 19a). This indicates that even the small amount of convective precipitation (i.e. latent heat release) generated in Simulation 1 (Fig. 14) is necessary for the development of the initial short wave. Figure 19a shows the beginning of the low-level circulation along the Florida coast in response to the upper-level short wave over Georgia. Thus, the model has correctly

ignored the initial weak disturbance and developed a surface cyclone as a result of the second, stronger short wave.

However, the model forecasts in Simulation 4 are in error by not forecasting the vigorous development. The predicted surface cyclone is too shallow and too slow. Figure 20 shows a 1001 mb low at 14/0000 with an inverted trough extending along the US coastline. Comparison with Fig. 6 demonstrates that precipitation was important, even at this early stage. The initial low is 3-5 mb too shallow and 475 km too far southwest. As one might expect, the rapid deepening of the surface cyclone is completely missed by the model in Simulation 4. The central pressure at 14/1200 is underforecast by 23 mb (not shown).

E. SUMMARY OF SIMULATIONS 1 - 4

Figure 21 summarizes the four numerical simulations. It is seen that the model never exhibits a "rapidly deepening" phase, but rather developed the cyclone at a constant rate, although predicted deepening rates between 13/0600 and 14/0600 (40 mb in 24 h) are certainly impressive. In contrast, the observed cyclone exhibited the rapid deepening in a 6 h period[3]. The fact that, at 14/0000, the first three simulations were ≈ 15 mb too deep and Simulation 4 was only 5 mb too shallow, seems to indicate that the role of convection was rather small up to this point. Still, the errors early in Simulation 4 show that precipitation did play a role in the early stages of development. Obviously, though, the importance of latent heat release in the explosively deepening phase cannot be ignored. To investigate this more closely, several diagnostic studies were performed on the model output and are discussed in section 6.

---

3. There is high confidence in the actual central pressure trace due to the aircraft and buoy measurments available.

F. OTHER OPERATIONAL FORECASTS

As mentioned in section 3, the NGM and Spectral models run at NMC produced very good operational forecasts in terms of position error (100 km at 48 h). However, the NGM was 16 mb too shallow in its central pressure forecast. The Spectral was much better (4 mb too deep). But it too was similar to the NORAPS model in that it gave a very poor 36 h forecast (Fig. 22). As with NORAPS, the Spectral model failed to resolve the multiple centers, and the central pressure of the low is 10 mb too deep. The 500 mb vorticity forecast is not as spurious as NORAPS, but since a smoothing procedure is applied to these operational charts, direct comparison is not possible.

A comparison of precipitation forecasts from the NGM and NORAPS shows that the NGM was much more conservative in its prediction (not shown). From 24 - 36 h, the NGM forecast a maxima of 1" (2.4 cm), while Simulation 1 predicted a maxima of 4.5" (10.9 cm) and Simulation 2 a maxima of 3.5" (8.5 cm). Precipitation forecasts for the Spectral model were not available.

VI. MODEL DIAGNOSTICS

In the previous section it was observed that while the 48 h prediction by the NORAPS model was very good in terms of central pressure, the 36 h forecast (valid at 14/0000) was 16 mb too deep. This was largely the result of intense convection early in the simulation. The model run with no precipitation showed only a small error in central pressure at 14/0000. This section will investigate the effects of convection in the model simulations. In all figures of model data, the actual sigma level values were used to construct cross sections and Skew-T diagrams.

A. TIME SECTIONS

Section 3 described the Kuo scheme of convection parameterization which is used in the NORAPS model. The effective result of convection is to transport latent heat and moisture from low levels (i.e., the PBL) upward. But before convection in the model begins, four criteria must be met (reviewed in Section 3).

It was already shown in section 5 that the convective precipitation was occurring in areas with convergence at 1000 mb, implying that the criteria for low-level moisture convergence had been met. To see if the other three criteria were correctly satisfied, time sections were constructed at ERICA drifting buoy locations in which intense convective precipitation was falling in the model. Figures 23 - 25 show the equivalent potential temperature, relative humidity, and mixing ratio time sections for Simulation 1 at 33°N 70°N (buoy 11369). The time sections clearly show that the Kuo scheme is accomplishing its goal. The profile of Θ_e indicates a deep layer (surface to 850 mb) of conditional instability due to cold air from the New England anticyclone flowing over the warm Gulf Stream waters. The air is also nearly saturated up to 650 mb (Fig. 24). Thus, the neces-

23

sary conditions for convection outlined in section 3 appear to exist. The potential temperature time section (not shown) indicates weak static stability below 850 mb with stronger stability above this layer. Thus, the conditional instability ($d\Theta_e/dz < 0$) in Fig. 23 is largely due to the moisture profile.

From charts of convective precipitation (see Figs. 14 and 15b), it was determined that very light precipitation from convection began in NORAPS between 12 and 18 h into the forecast simulation at the 33°N 70°W grid point. From hours 18 to 24, approximately 5 cm of precipitation fell at this location. Figures 23 and 25 indicate that the convective parameterization began to take effect after about the 12 h mark, since the upper levels (700 - 500 mb) begin to moisten creating a conditionally neutral layer aloft as shown by the vertical Θ_e lines. The low-level conditional instability also begins to be removed after 12 h. A sharp jump in the moisture profile occurs 18 h into the simulation (Fig. 25), the same time at which the significant convective precipitation begins. The entire column from the surface to 500 mb is nearly neutral by this time. The low-level moisture has been moved upwards as evidenced by the pocket of greater than 90% humidity in Fig. 24 and the drier 70% contours below. After hour 21, the upper levels begin to dry rapidly (Fig. 24) indicating the intrusion of drier air from the west, while the low levels begin to moisten as evidenced by the 90% contour, setting up another conditionally unstable situation. The cause of this moistening is two-fold: evaporation of the precipitation into the drier low-level air and a shift in the low-level wind direction from northeasterly to southerly (not shown) as the warm front passes by, advecting more moist air from the south.

Figure 26 is a north-south cross section from a study by Reed and Albright (1986) of an explosively deepening cyclone in the eastern North Pacific. Note how the equivalent potential temperature contours are oriented vertically where convection is occurring. The Θ_e lines in the current study (Fig. 23) are also oriented vertically after 18 h as significant convective precipitation began to fall. In the cold air to the north (left) in Fig. 26, potential

24

instability is indicated by the $d\Theta_e/dz < 0$ up to 700 mb. This is similar to the left side of Fig. 23 where the cold air from the New England anticyclone is moving over the warm water.

A comparison between the air temperatures measured by the buoy and the analysis temperatures at each model level was performed (not shown). This comparison revealed that the lowest model level (21 m) was 1.4°C <u>warmer</u> than the buoy. Considering that the New England anticyclone was advecting cold air over the warm water, one would expect to find colder temperatures above the surface layer. This anomaly was also observed at other buoy locations in the same region. The temperature difference became larger as the simulation progressed. The cause of this warming is most likely the warm ocean waters. But a comparison of the measured sea-surface temperatures (SST's) and the model SST analysis showed good agreement. This appears to imply that the NORAPS model might possibly be modifying the cold air too rapidly. This warming by the warm ocean destabilizes the atmosphere, as seen in Fig. 23.

Similar time sections were constructed for Simulations 2 - 4. It was pointed out in section 5 that Simulations 2 and 3 did not differ significantly from Simulation 1 in terms of the sea level pressure forecast, but that the convective and stable precipitation predictions were different. The precipitation charts indicate that the total rainfall at the diagnostic grid point for Simulation 2 (KUO74) was much less than Simulation 1 (KUO65), ($\approx$ 1.5 cm compared with $\approx$ 5.0 cm). The KUO74 scheme intentionally decreases the moistening when saturation is nearly reached, which decreases the amount of precipitation. But as the moistening is decreased, the scheme correspondingly increases the sensible heating. Additionally, stable precipitation is increased in the KUO74 simulation. Thus, the overall heating profile is nearly identical to Simulation 1 (KUO65).

This difference between the two convective parameterization schemes is shown in the time sections. Figures 27 and 28 are the equivalent potential temperature and mixing ratio

time sections for Simulation 2. Comparing these to Figs. 23 and 25, both simulations look nearly identical for the first 15 h. But the conditional instability is removed more quickly in Simulation 1 as shown by comparing the vertical Θ_e contours in Figs. 23 and 27. The moistening process is also slower in the second simulation, which is noted by comparing the 8 g/kg contour in Figs. 25 and 28. The first simulation (KUO65) moistens the column more quickly than Simulation 2 (KUO75), which removes the conditionally unstable layer faster and causes more precipitation. Thus, the intense convection in Simulation 2 is delayed as compared to Simulation 1.

As would be expected, the time sections for Simulation 4 (no precipitation) are considerably different from the other three simulations. Figures 29 and 30 show the equivalent potential temperature and the mixing ratio respectively. The initial low-level conditional instability exists as in Simulations 1 and 2. However, with the convective parameterization turned off, the model has no way to relieve this instability. Instead, the conditionally unstable layer deepens. Also, note the marked differences in the moisture profiles of the two simulations, with Simulation 4 indicating only a small amount of moistening in the low levels, and none aloft. During this period (15 to 27 h), the low-level winds shift from northeasterly to easterly, again suggesting that advection was the primary cause of the moistening observed in this simulation.

B. IMPORTANCE OF INITIAL CONDITIONS

From a qualitative analysis, the convective parameterization scheme appears to be performing correctly. The model atmosphere possesses the necessary conditions to cause convection and the Kuo scheme relieves the potential instability by transporting low-level latent heat and moisture upward. However, the high values of convective precipitation noted in section 4 indicate that the model is performing incorrectly in its prediction of

convection. Since the predicted temperature and moisture play a large role in the cumulus parameterization, these fields are further investigated.

The time sections in section 5a were coincident with a drifting buoy in the location of predicted convective precipitation. However, this did not allow for comparison with actual data at levels above the surface. In order to achieve this, a cross section was constructed using four Air Force dropsondes taken at 13/0000. Figure 31 is the equivalent potential temperature and mixing ratio cross sections along the line indicated on Fig. 14. The low-level potential instability created by the advection of cold air over warm water is clearly indicated by the "tongue" of low Θ_e values near 900 mb. The corresponding NORAPS 12 h forecast cross section for Simulation 1 is shown in Fig. 32. NORAPS also possesses a layer of potential instability. From Fig. 14 it is noted that convective precipitation has already been occurring in the region of the cross section. Thus, some of the instability has already been relieved, especially in the region between dropsonde 3 and 4. A similar cross section 6 h earlier (not shown) does in fact show that the model atmosphere was more unstable.

Comparison of Figs. 31 and 32 reveals a disturbing fact: the model atmosphere is much moister in the low levels, typically by 2 g/kg. Analysis and 6 h cross sections (not shown) show little change in the moisture field. Thus, it appears NORAPS was initialized with a poor moisture field. As was previously mentioned, NORAPS does not perform an actual moisture analysis. Instead, it uses its previous 12 h moisture forecast as the analysis. Obviously, this could result in a situation such as that in the present study.

Figure 33 shows a comparison of the actual Air Force dropsonde 3 and the corresponding NORAPS 12 h forecast sounding (denoted by AF03 in Figs. 31 and 32). While the overall soundings look similar, closer inspection reveals that NORAPS is both moister and warmer than the observed atmosphere. Also note that the observed inversion between 850 - 700 mb (Fig. 33a) is not predicted by the model (Fig. 33b). The result is a more

27

unstable sounding in the model, as indicated by the stability indices. Similar soundings for all other (18) dropsondes show that the model is more unstable than the real atmosphere. This is somewhat surprising since the actual atmosphere "looked" more unstable than the model in the Θ_e cross sections (Figs. 31a and 32a). Also, convective activity in this region had already served to stabilize the model atmosphere somewhat. Clearly, the model is not doing a good job of predicting the temperature and moisture fields in the lower levels. And since the analysis fields (not shown) are even more unstable, it is suspected that the initial NORAPS fields poorly represented the actual atmosphere.

In order to determine if the poor representation of the temperature and moisture was due the lack of data, comparisons were made between the model and the 12/1200 soundings (not shown) at West Palm Beach, FL (72203). Charleston, SC (72208). Cape Hatteras. NC (72304), Nassau, Bahamas (78073). and Bermuda Island (78016). In all cases but Bermuda, the model analysis was nearly identical to the observation data. As with the Air Force dropsondes. NORAPS was too warm and moist at Bermuda. Therefore it appears that the NORAPS analysis gives a correct depiction of the atmosphere when data are available, but may be poor over the data sparse ocean regions. Model 12 h forecast errors are passed on to the next analysis through the first guess field if there is no data to refute it. Thus, a poor 12 h forecast can result in a poor analysis.

It was mentioned in section 3 that for the present study, four 12 h forecasts had been made in order to simulate the update cycle in an operational environment. Hodur (1987) showed that the inclusion of a 12 h update cycle improved NORAPS forecasts. Thus, the NORAPS analysis could differ from the global model (NOGAPS) analysis because of the use of the previous 12 h forecast as the first guess field. Also in section 3 it was pointed out that neither NORAPS nor NOGAPS analyze moisture. Rather, the initial moisture field for a model simulation is the previous 12 h forecast. Surface temperatures measured by ships and buoys are also not used in the analysis.

To investigate the impact of these procedures, Fig. 34 compares the 2 m air temperature analysis from NORAPS (34a) and NOGAPS (34b) with actual ship and buoy observations. The ERICA buoy data shown in this figure was not used in the model analysis. Note that south of 35°N, NORAPS (Fig. 34a) is generally warmer than the observations, by as much as 6°C. The NOGAPS analysis (Fig. 34b) shows much less detail in the temperature field, especially near the coastline. However, the analysis appears to be in much better agreement with the observed temperatures, although the ERICA buoys near 32°N are still colder than the analysis. Since the temperature is not analyzed directly by either model, these differences are largely a result of the previous 12 h forecast.

Figure 35 is the initial 1000 mb vapor pressure (moisture) fields for the NORAPS (35a) and NOGAPS (35b) models. The NORAPS model again shows more detail in the 1000 mb moisture field than does the global model. However, the regional model is considerably moister, especially south of 35°N (note the location of the 15 mb contour as it crosses 70°W). Comparison of actual moisture values at 12/1200 (not shown) to the NORAPS and NOGAPS analyses show that NOGAPS is more much more realistic, and may in fact be slightly too dry. The better moisture analyses in NOGAPS are actually better 12 h forecasts, since there is no actual analysis of moisture.

The causes for the differences between the NORAPS and NOGAPS low-level temperature and moisture fields are beyond the scope of this study. As mentioned in section 6a, one possibility is that as the continental polar air moves over the Gulf Stream waters, the NORAPS model is modifying the air too rapidly, thus making it warmer and moister in the low levels. The drier NOGAPS fields might also be the result of different model physics, such as the use of the Arakawa-Schubert (1974) scheme for convection (Rosmond[4].

---

4. Dr. Thomas E. Rosmond is the head of the Prediction Systems branch of the Naval Oceanographic & Atmospheric Research Laboratory, Atmospheric Directorate, Monterey, CA.

personal communication), rather than the Kuo (1974) scheme used in the NORAPS model for the current study.

C. SIMULATION WITH NOGAPS INITIAL FIELDS

In order to test the hypothesis that the excess temperature and moisture in the NORAPS initial fields are adversely effecting the model simulations, a fifth simulation was carried out where the model was initialized with the global analysis fields (i.e., no regional update cycle). The model for the this simulation used the KUO74 convection scheme. Additionally, minor improvements were made to the boundary conditions, but these have relatively small influence on the forecast (Liou, personal communication).

A subjective comparison of the NOGAPS surface and 500 mb analyses with the fields used to start the first four simulations showed some minor differences, but these were primarily out of the region of interest. The important weak disturbance over Florida was depicted in both analyses by the $8\ s^{-1}$ vorticity contour. Thus, the major difference between this simulation and Simulation 2 is the initial *low-level temperature and moisture fields.*

The cumulative convective precipitation from 12 to 18 h is shown in Fig. 36. Comparing this with Fig. 19 from Simulation 2, it is seen that the drier initial moisture field has had an effect on the convective precipitation, both in amount and distribution. The corresponding sea level pressure fields (not shown) differ only by 1 mb. Likewise, the 500 mb fields show little difference, although the new simulation moves the short wave somewhat faster. Still, the model is developing the wrong initial low. But by hour 30 (Fig. 37), an improvement is noted. Since the initial low at this time is not as deep as in Simulation 2 (998 mb vs 991 mb in Simulation 2, not shown), NORAPS attempts to develop the secondary low to the northwest. The subjective analysis from Chalfant (1989) at this time (not shown) shows the observed second low in good agreement with the forecast position

and central pressure. However, the primary low has a large error in both position and central pressure, although it is closer to the observed 1002 mb value than Simulation 2.

By 14/0000, the two simulations are considerably different. Figure 38 is the surface pressure forecast for Simulation 5. (The forecast by Simulation 2 at this time is identical to Simulation 1 (Fig. 16) and is thus not shown). The 989 mb low is still in error by 7-9 mb. But this is a considerable improvement over Simulations 1-3. Note that the low in Simulation 5 is moving much more rapidly. Anthes et al. (1983) point out that latent heating reduces the cyclone's speed of movement. As Table 2 indicates, this simulation produced much less precipitation, thus agreeing with this finding.

Table 2 also reveals the effect of the reduced precipitation. The 48 h central pressure forecast is 971 mb, in close agreement with the observed 968 mb. Note that it appears that the amount of predicted deepening is related to the total amount of precipitation, not the convective or stable amounts alone. KUO74 reduced the amount of convection from that of KUO65, but the stable precipitation increased resulting in a similar amount of latent heating. Only when both types of precipitation were reduced was the deepening rate improved (see Fig. 21).

Therefore, it appears that the initial low-level temperature and moisture fields play a significant role in the development of the cyclone. The cumulus parameterization is sensitive to small changes in the moisture field and correspondingly varies the amount of precipitation, and thus the amount of latent heat release. The result is a difference in both the track and intensity of the predicted cyclone, with both improved over the earlier simulations with the NORAPS update cycle. The exact cause of the excessive heat and moisture in the NORAPS analyses is beyond the scope of the current study, but is most likely linked to the boundary layer parameterization (mixing) and vertical grid resolution (see Table 1). Again it should be noted that this is just one case and that similar studies may show results which support or contradict these findings.

VII. SUMMARY AND CONCLUSIONS

Considerable work has been done in the area of numerical prediction of rapid oceanic cyclogenesis. Several studies have focused on the latent heating aspect as the key mechanism controlling the deepening rate. Yet, in nearly all of these studies, the deepening rate was typically less than observed. While the operational NORAPS 48 h forecast valid at 14/1200 UTC appeared quite good, a closer inspection reveals that the intermediate forecasts were rather poor, with NORAPS over-forecasting the development of the ERICA IOP-2 cyclone.

An investigation into this numerical forecast showed that the NORAPS model incorrectly developed a low too early in the forecast due to problems in the convective parameterization. Furthermore, the development of this low was too rapid, with an over-forecast central pressure of 18 mb at 14/0000 UTC. Unrealistically large amounts of convective precipitation appear to be responsible for the overdevelopment, as the convection generated spurious amounts of vorticity at 500 mb with no appreciable change in the height pattern.

Varying the cumulus parameterization scheme decreased the amount of convective precipitation, but since the stable precipitation correspondingly increased, this resulted in very little change in the surface pressure and 500 mb height forecasts. Danard (1985) found a direct correlation between the maximum amount of convective precipitation and the predicted deepening. This fact was not observed in the present study. Kuo and Low-Nam (1990) emphasized the importance of warm frontal stable precipitation to the rate of deepening. They found that the simulations using the Arakawa-Schubert convective parameterization were superior to those using Kuo. They concluded that this was primarily the result of the former scheme precipitating much less in convection than the latter,

leaving more available moisture for the stable precipitation. Stable precipitation is typically more efficient than convective precipitation at deepening a cyclone since it occurs lower in the atmosphere. As Anthes et al. (1983) points out, the lower the level of maximum heating, the more intense the resulting surface cyclone. For the current study, the total amount of precipitation was the only link to the predicted deepening rate. However, the importance of the location of the precipitation, both horizontal and vertical, cannot be overlooked.

In order to verify that the latent heat release was the cause of the overforecast deepening, a simulation with no precipitation was run. This alteration dramatically slowed the development of the initial cyclone, but failed to adequately predict the explosive deepening which was observed. The underprediction of the low prior to the rapid deepening phase indicates that precipitation was important in the early stages.

Detailed diagnostics were performed to analyze the role of the convective precipitation. It was determined that the cumulus parameterization scheme was working properly. However, comparisons of model analyses and forecasts to observed data indicate that the model was poorly initialized, especially in low levels over the ocean, resulting in a great deal more potential instability. The comparisons with ERICA dropsondes also showed that the model forecasts were too warm in the low levels, which may be a result of a poor surface flux parameterization. It was recognized that the lack of a moisture analysis also might be partly responsible for the poor initialization. In order to investigate this, a fifth simulation was conducted which used the global analyses as initial fields. These global fields were found to be drier and more realistic. The resulting forecasts were improved, both in sea level pressure and precipitation amounts, although the model still developed the wrong low, and then failed to deepen it enough.

A comparison with two NMC models, the Nested Grid Model and the Global Spectral Model, showed similar deficiencies to those found in NORAPS. Both models developed

33

the initial low and failed to resolve the secondary development off the Virginia - North Carolina coastline. While the NGM model was 16 mb too shallow at 14/1200, the spectral model actually overforecast the development by 4 mb, similar to the operational NORAPS forecast. Both models did very well in predicting the 48 h location of the cyclone.

This study agrees with previous findings on the importance of latent heating in the development of wintertime oceanic extratropical cyclones. The quality of numerical forecasts relies on the quality of the initial data. In data sparse regions, model forecast errors often propagate through successive forecasts via the first guess field unless there are available data to correct the analysis. Parameterizations for convection and surface fluxes are very sensitive to details in the model atmosphere. Incorrect specification of this initial atmosphere can have an adverse effect on the forecasts even if the parameterization schemes are correct. Thus, the common lack of data is an important problem in the correct prediction of rapidly developing cyclones.

Since the initial moisture field appears to have had a large effect on the NORAPS forecasts, future work should be done in this area. The incorporation of an actual moisture analysis, rather than the previous 12 h forecast, could have a significant impact on explosive cyclogenesis forecasting. Additionally, it was noted that the low-level temperatures in NORAPS were often too warm in data sparse regions, further adding to the potential instability in the model. The current study used only those observations which were operationally available at the time of IOP-2. The extra buoy, rawinsonde, and dropsonde data collected as a part of ERICA should be integrated into the NORAPS analyses to investigate the importance of these data in numerical forecasting.
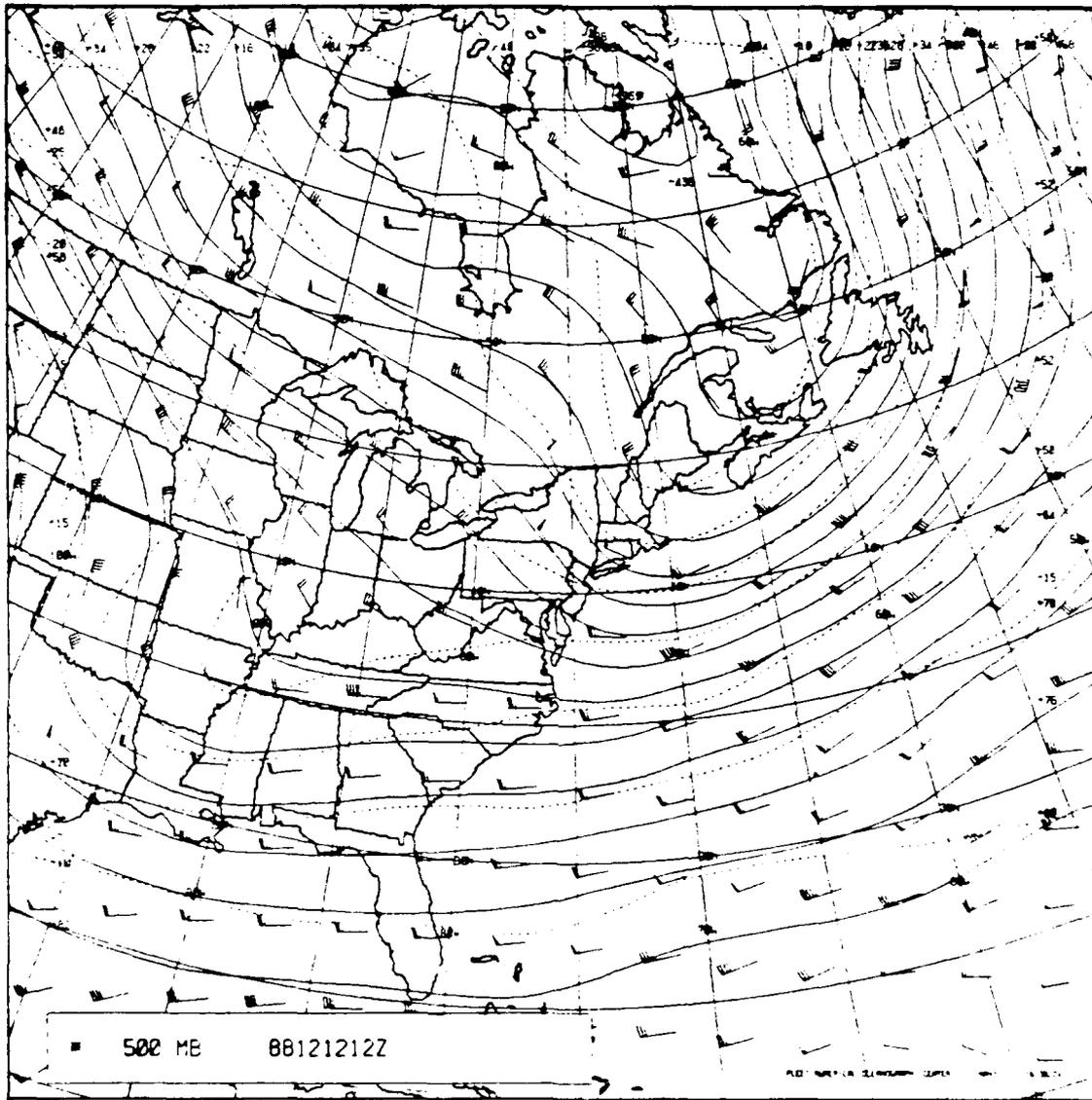
Fig. 1. FNOC 500 mb analysis for 1200 UTC 12 December 1988. Geopotential height (solid) is in dekameters (+64 represents 564 dam) and temperature (dashed) is in °C.
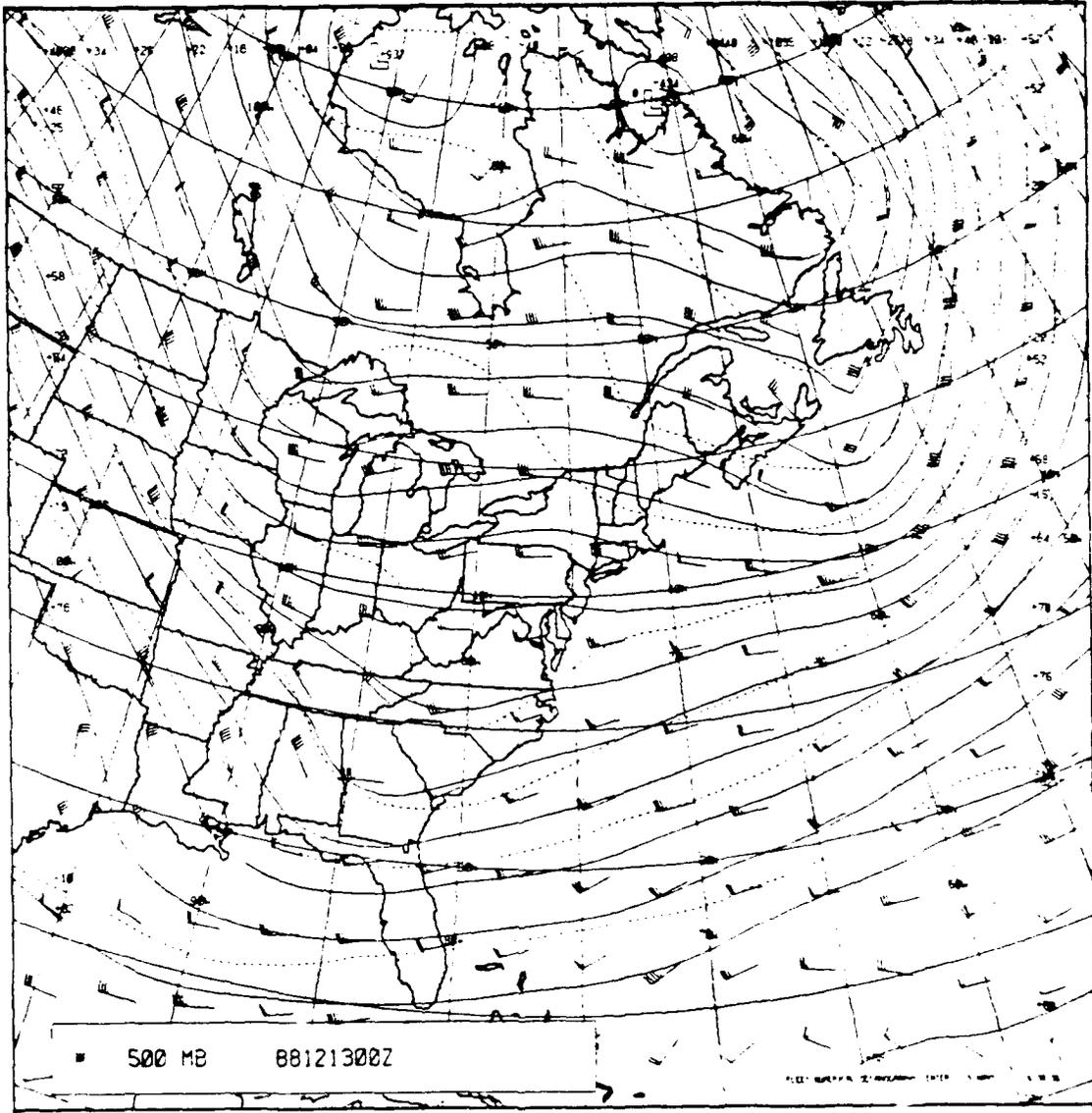
Fig. 2. As in Fig. 1 except for 0000 UTC 13 December 1988.
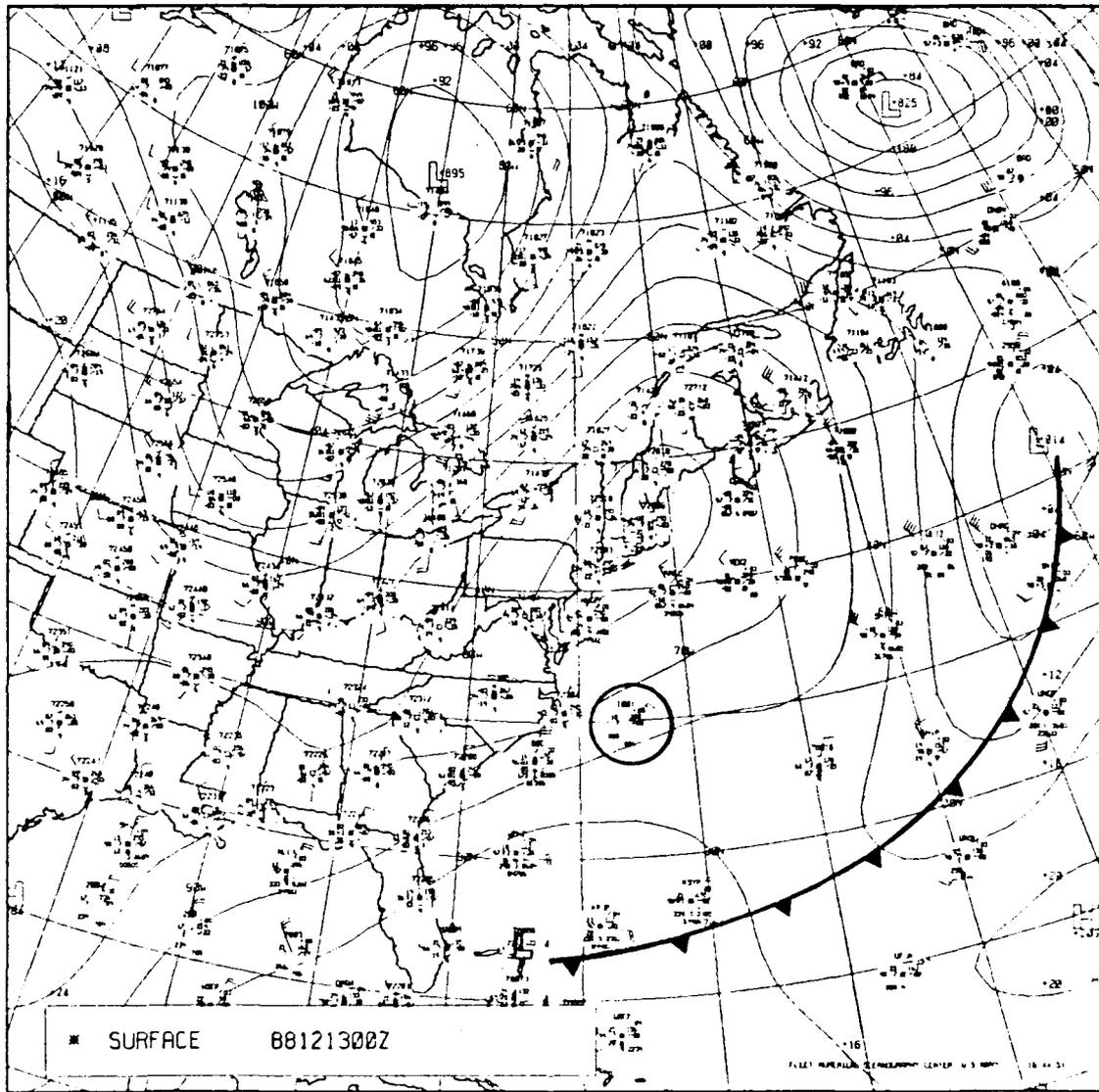
Fig. 3. FNOC surface analysis for 0000 UTC 13 December 1988. Sea level pressure contours are in mb minus 1000 mb (+20 represents 1020 mb). Surface report winds are in kt and temperatures are in °C. See text for explanation of circled buoy.
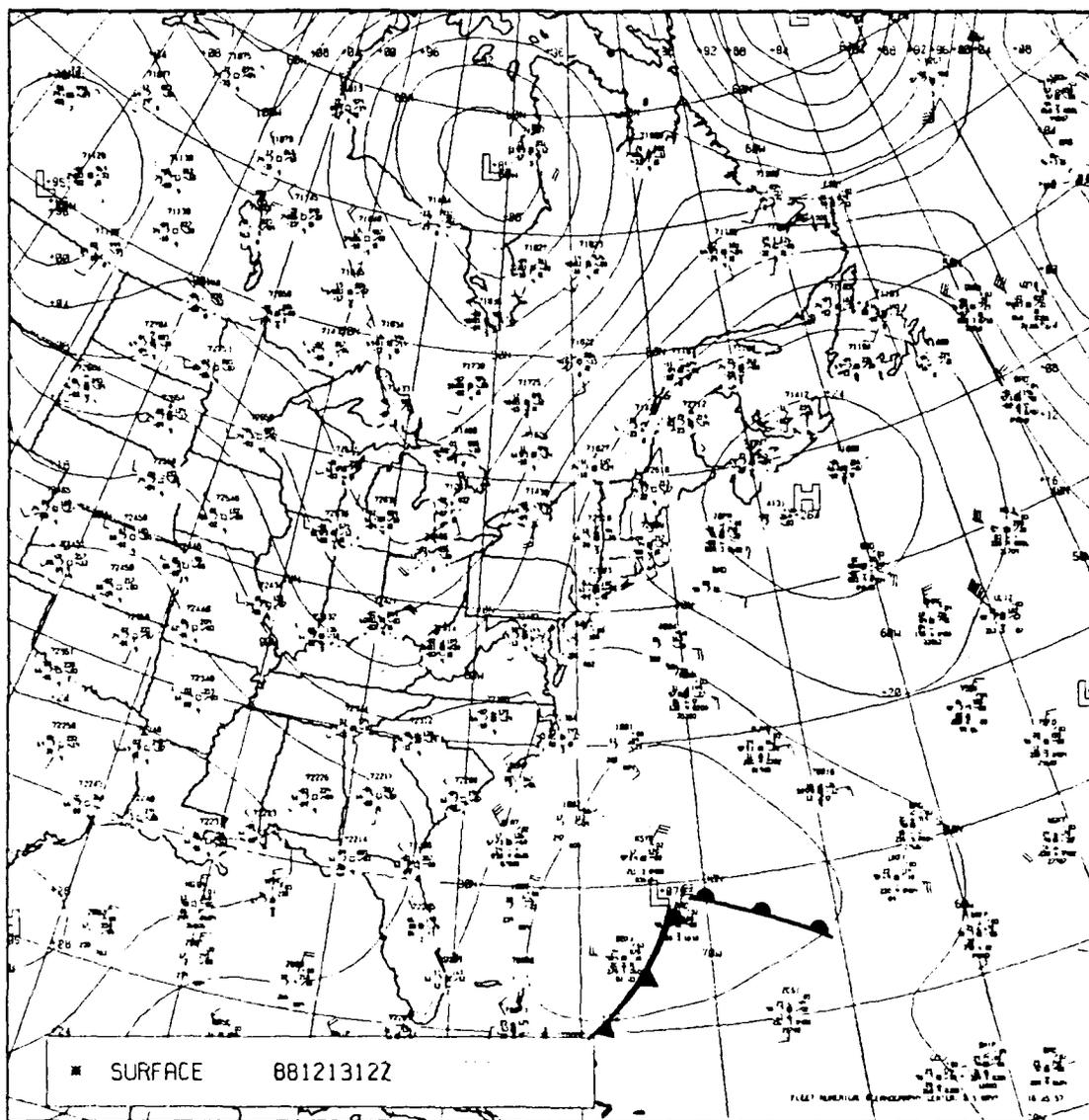
Fig. 4. As in Fig. 3 except for 1200 UTC 13 December 1988.
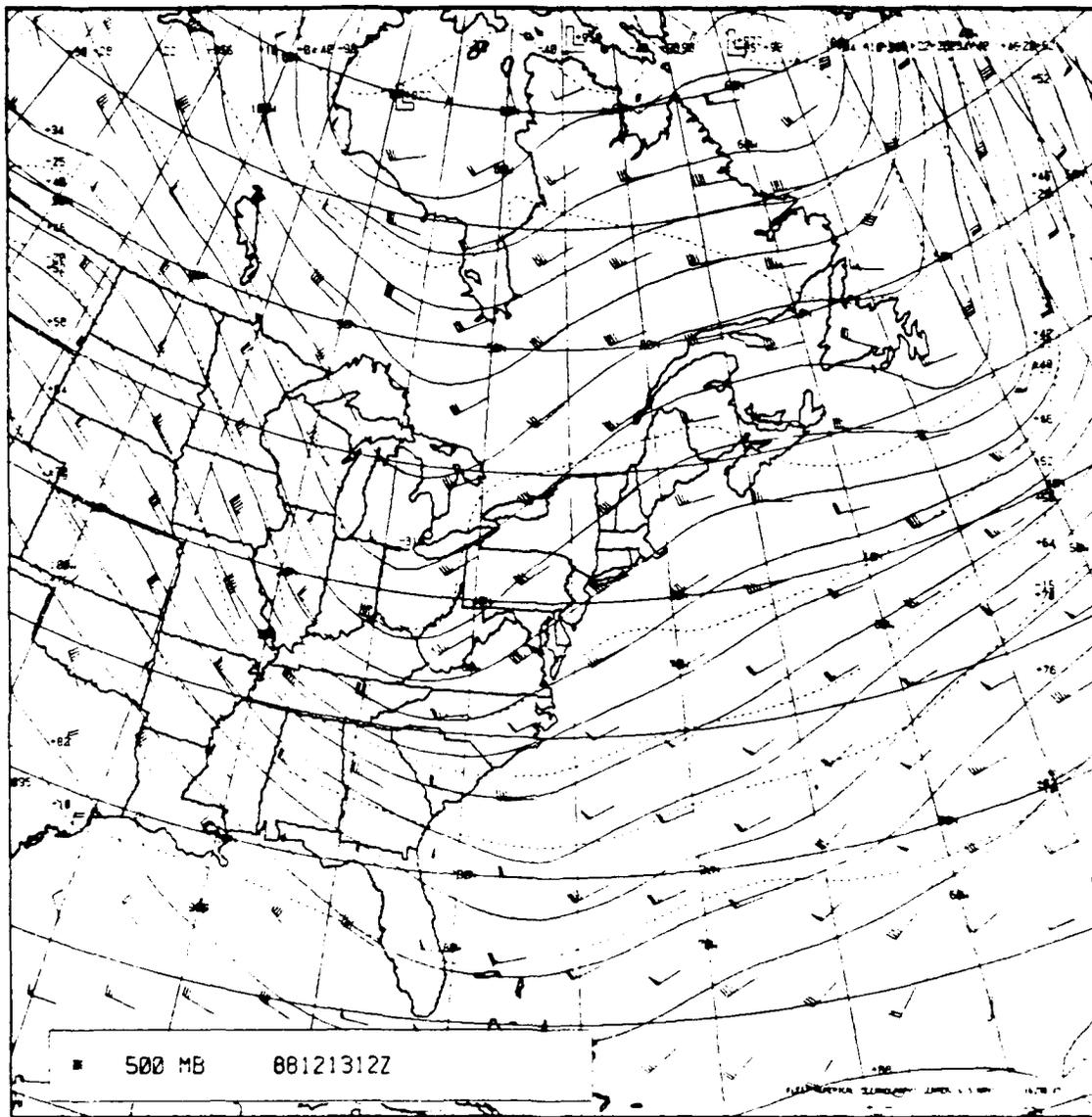
Fig. 5. As in Fig. 1 except for 1200 UTC 13 December 1988.
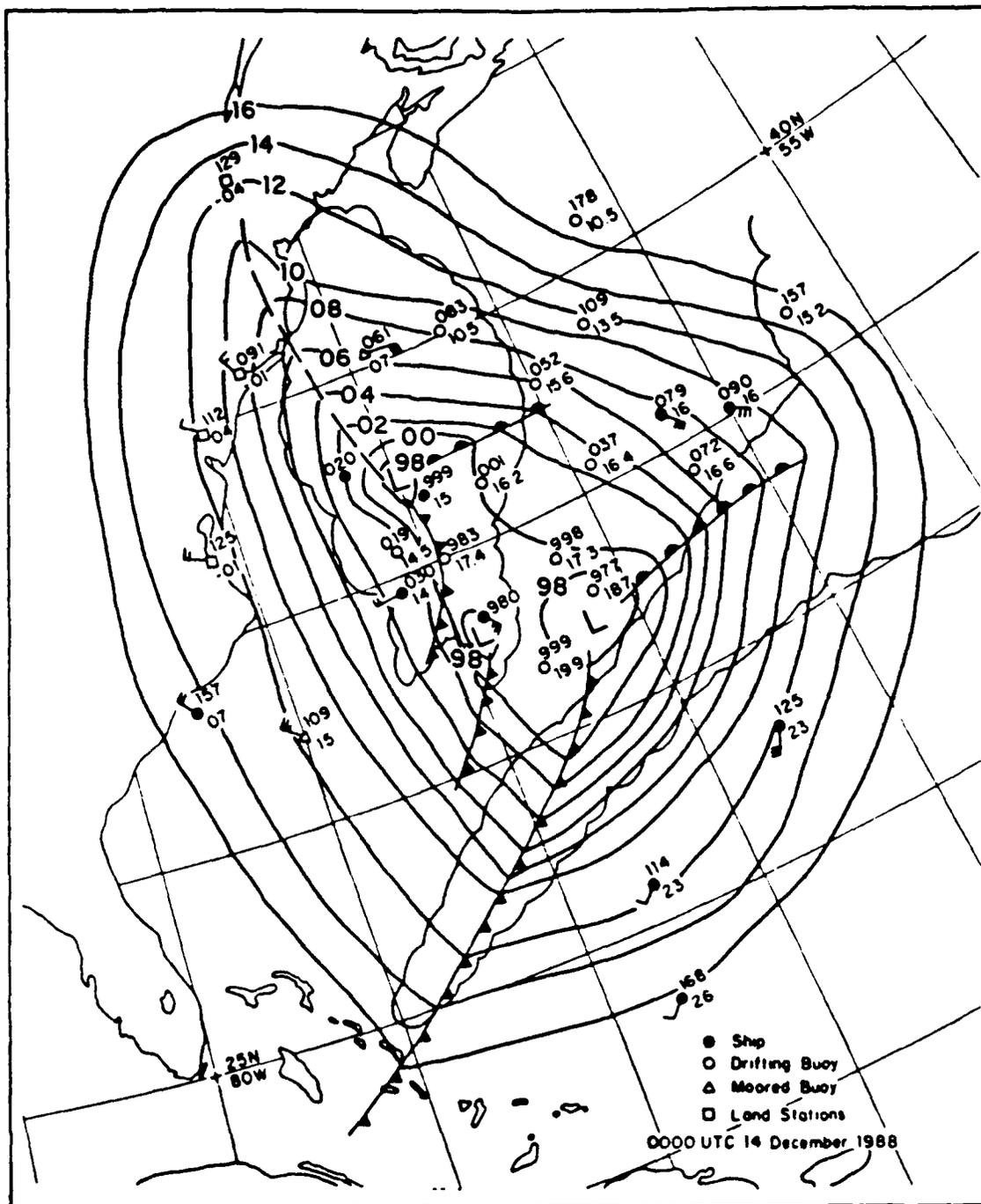
Fig. 6. Subjective surface analysis for 0000 UTC 14 December 1988. Surface pressure contour interval is 2 mb. Surface observations are of sea level pressure (125 = 1012.5 mb), temperature (in °C) and winds (in kt). From Chalfant (1989).

40
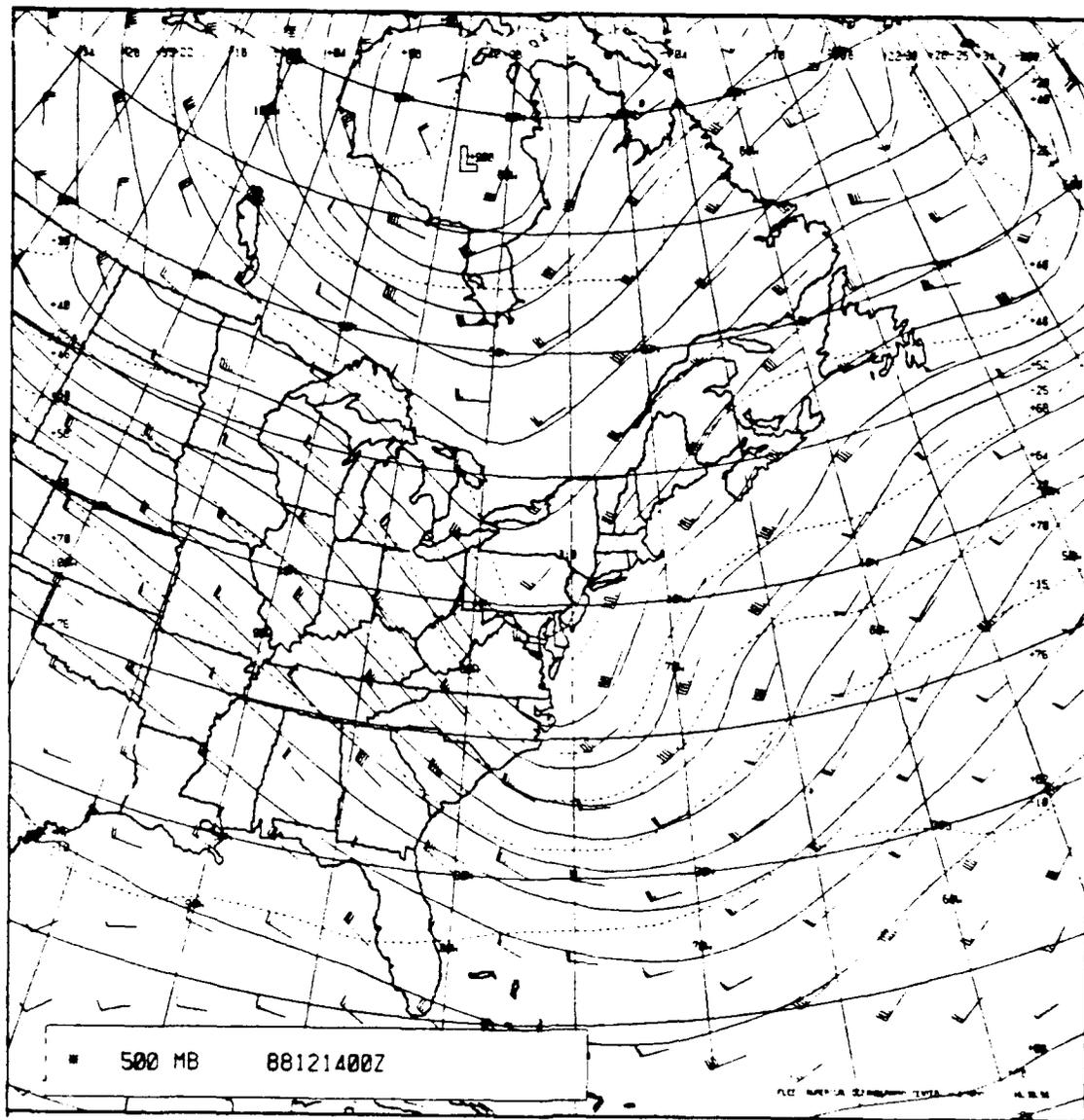
Fig. 7. As in Fig. 1 except for 0000 UTC 14 December 1988.
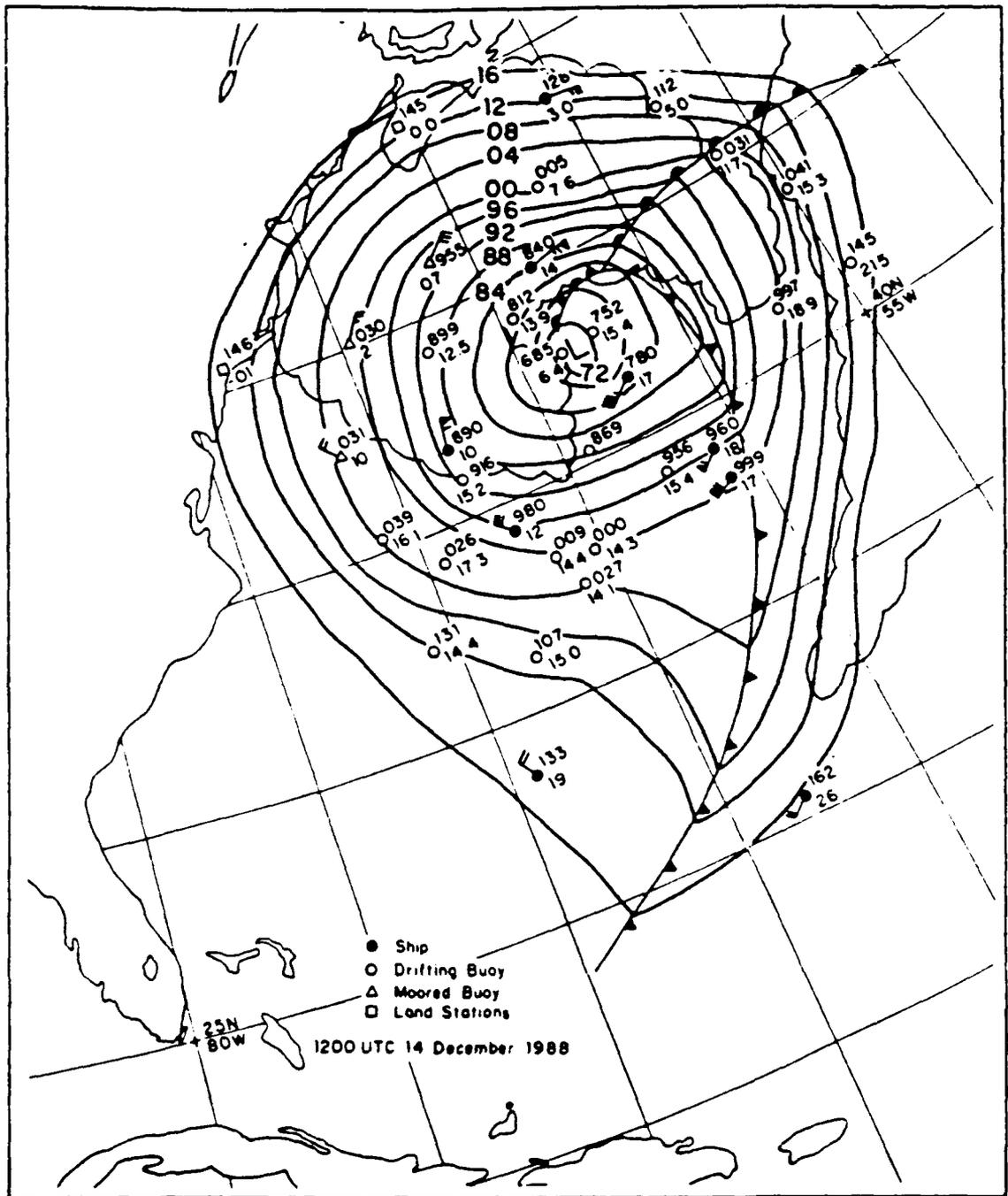
Fig. 8. As in Fig. 6 except for 1200 UTC 14 December 1988.
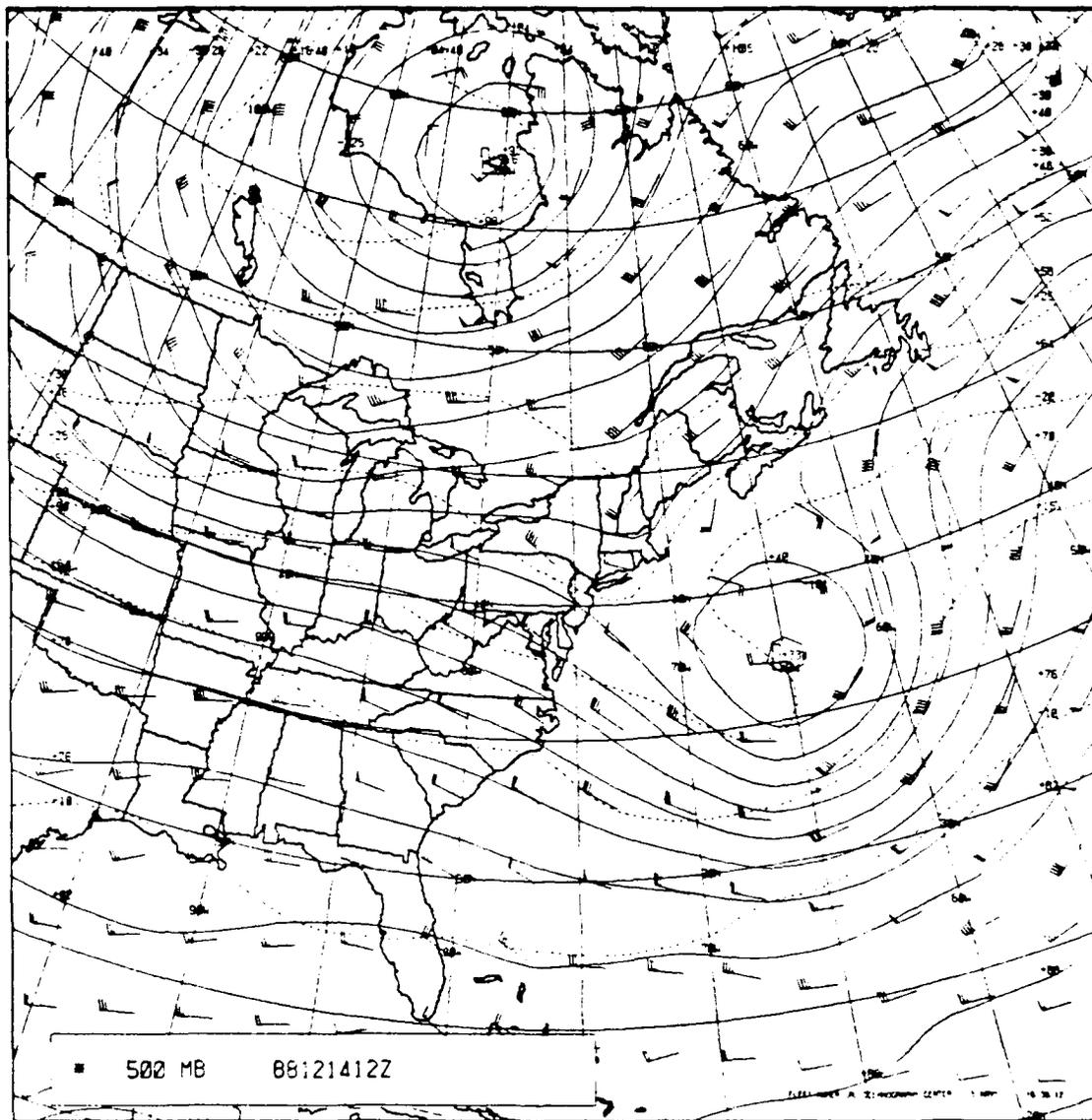
Fig. 9. As in Fig. 1 except for 1200 UTC 14 December 1988.

43
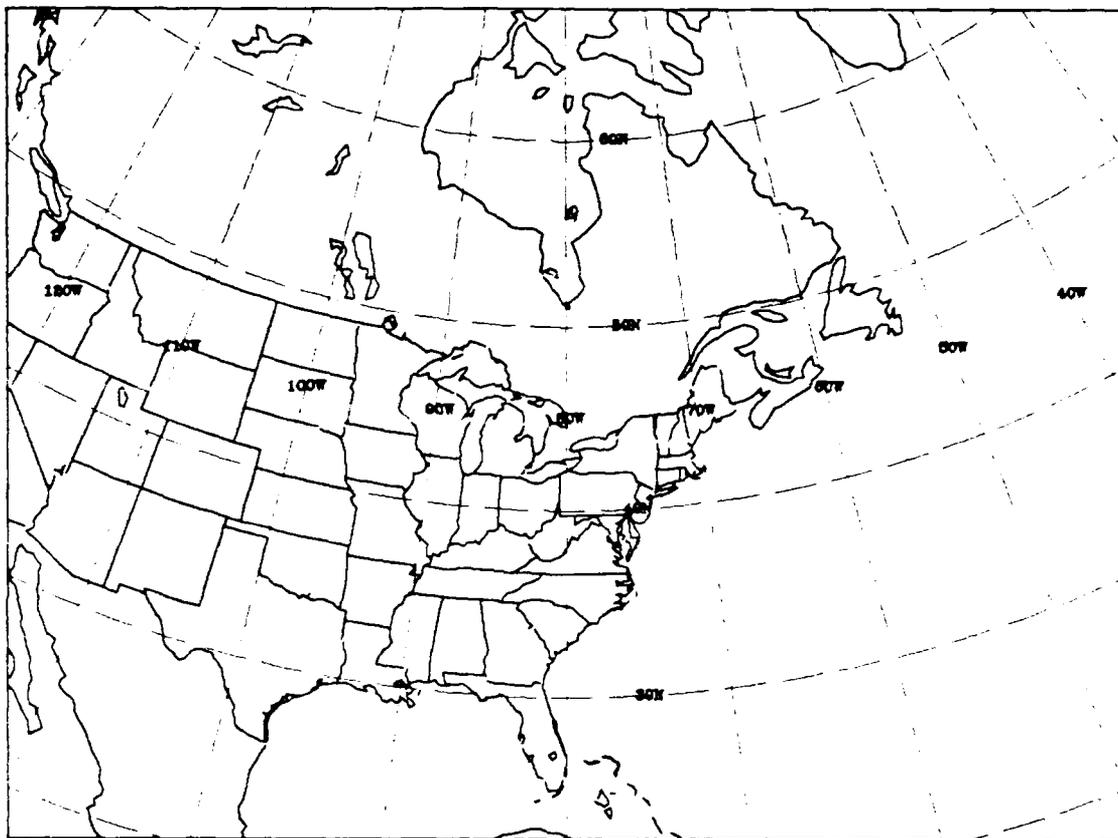
Fig. 10. NORAPS model domain for the current study.
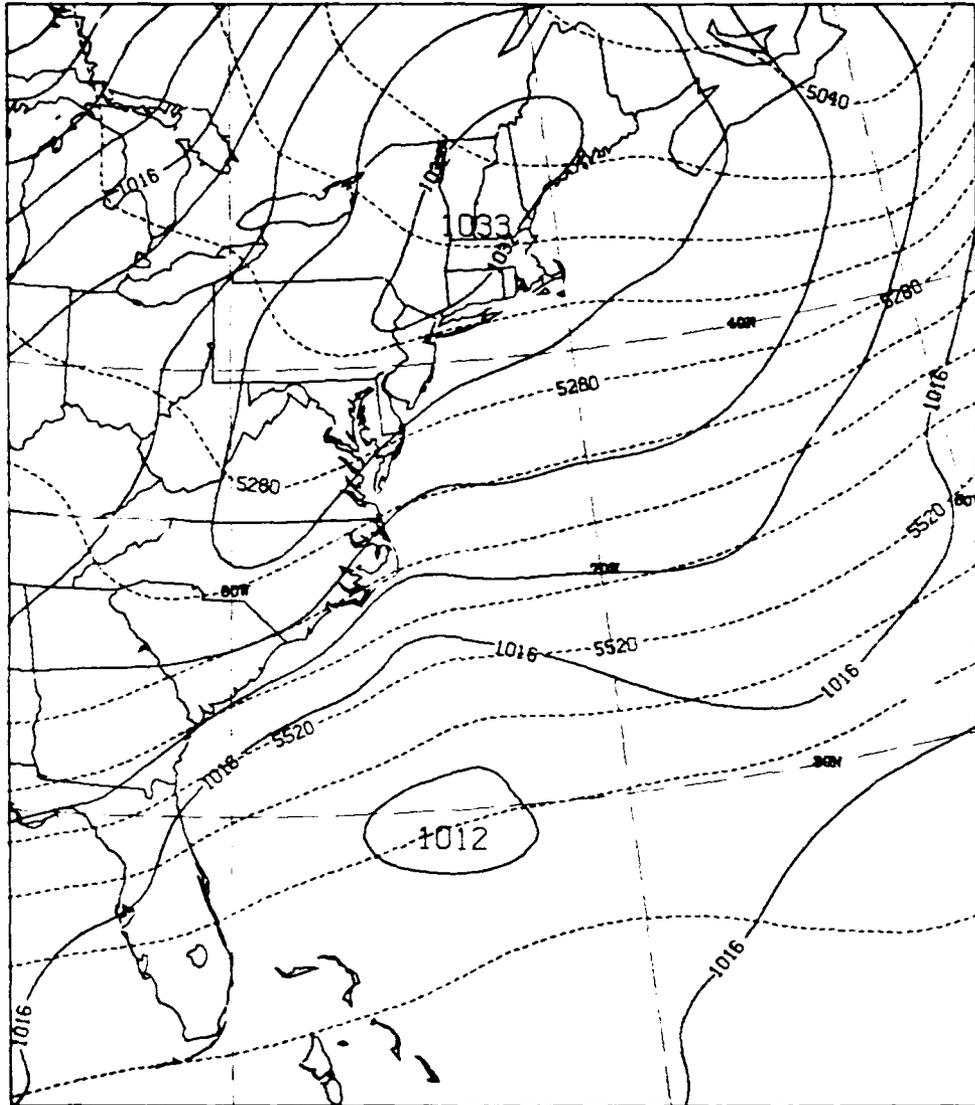
Fig. 11. 12 h forecast of sea level pressure (contour interval 4 mb) and 1000-500 mb thickness (dashed, contour interval 60 m) for Simulation 1.
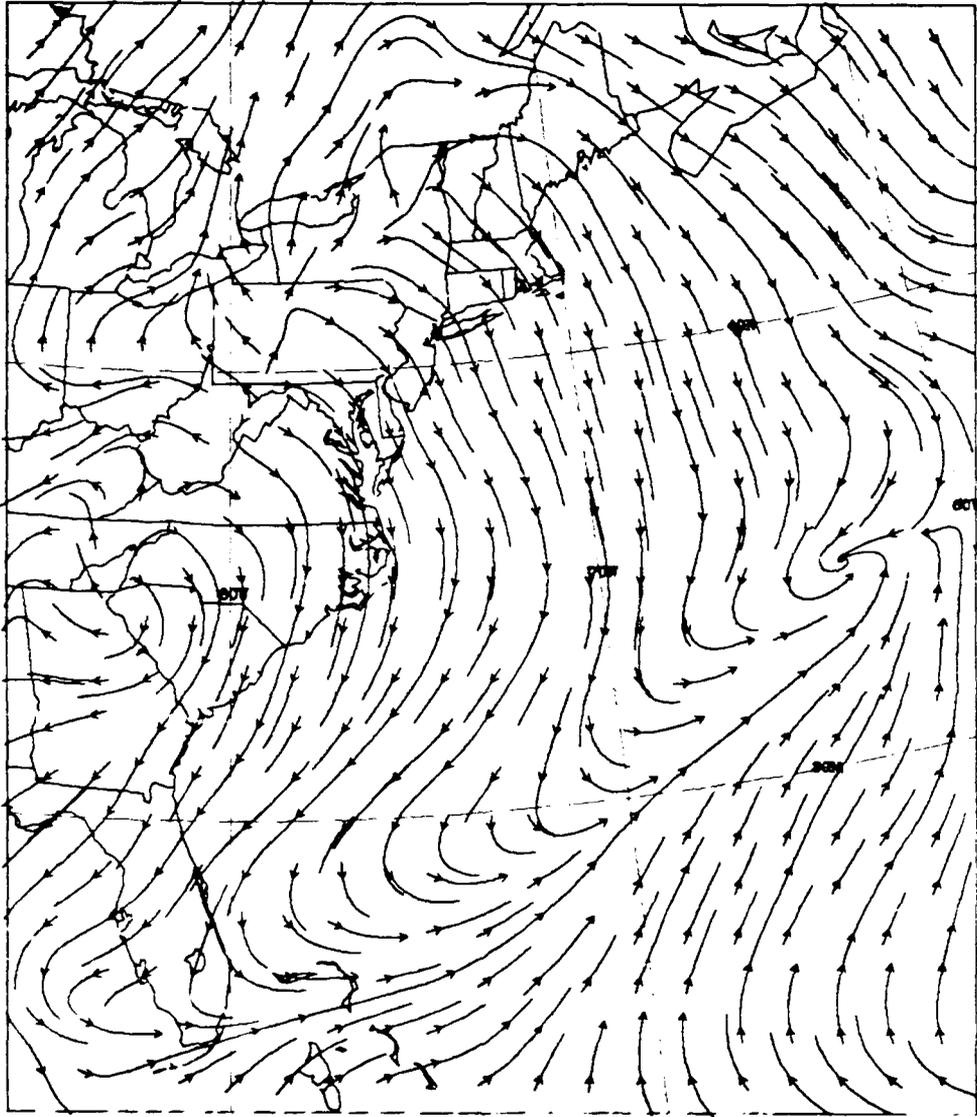
Fig. 12a. Initial 1000 mb streamlines for Simulation 1.
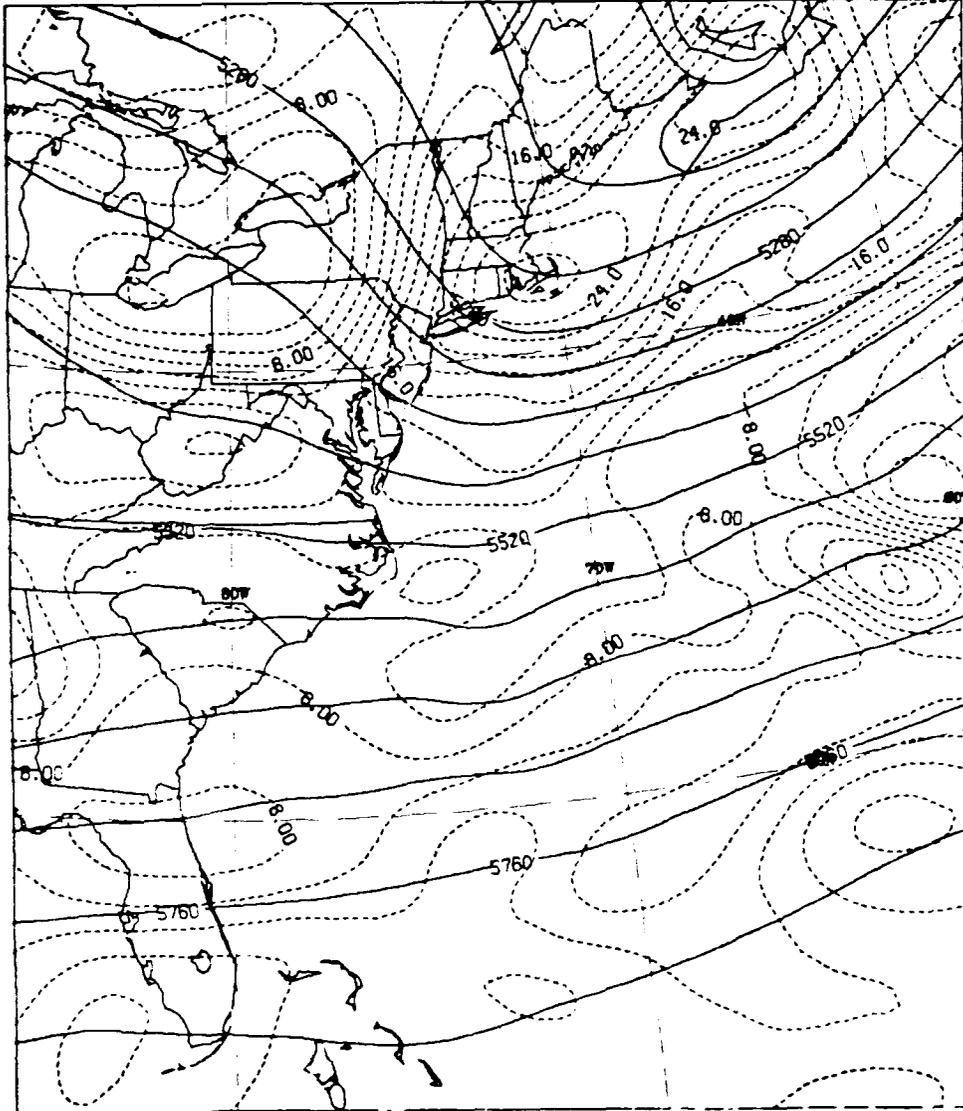
Fig. 12b. Initial 500 mb geopotential heights (contour interval 60 m) and absolute vorticity (dashed lines, contour interval 2 s^{-1}) for Simulation 1.
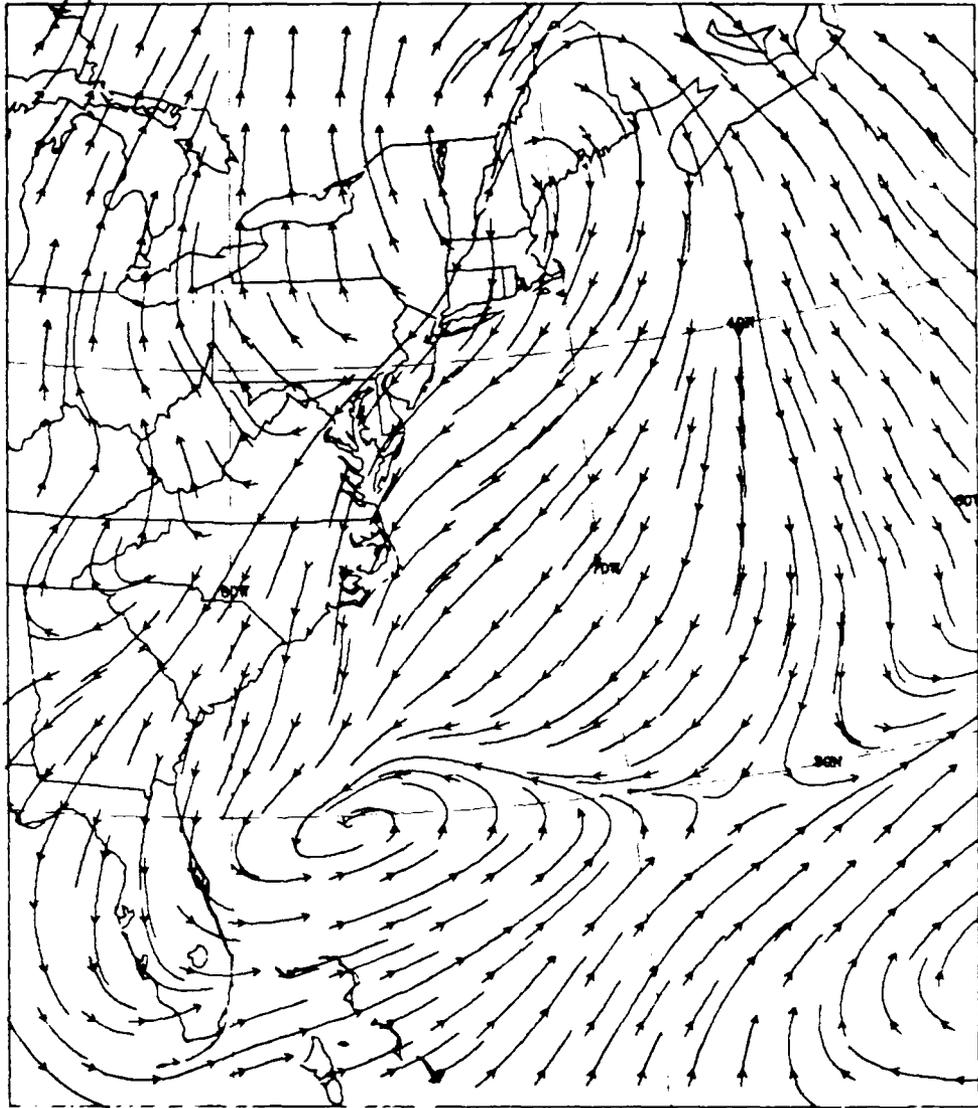
Fig. 13a. As in Fig. 12a except for 12 h forecast.

Fig. 13b. As in Fig. 12b except for 12 h forecast.
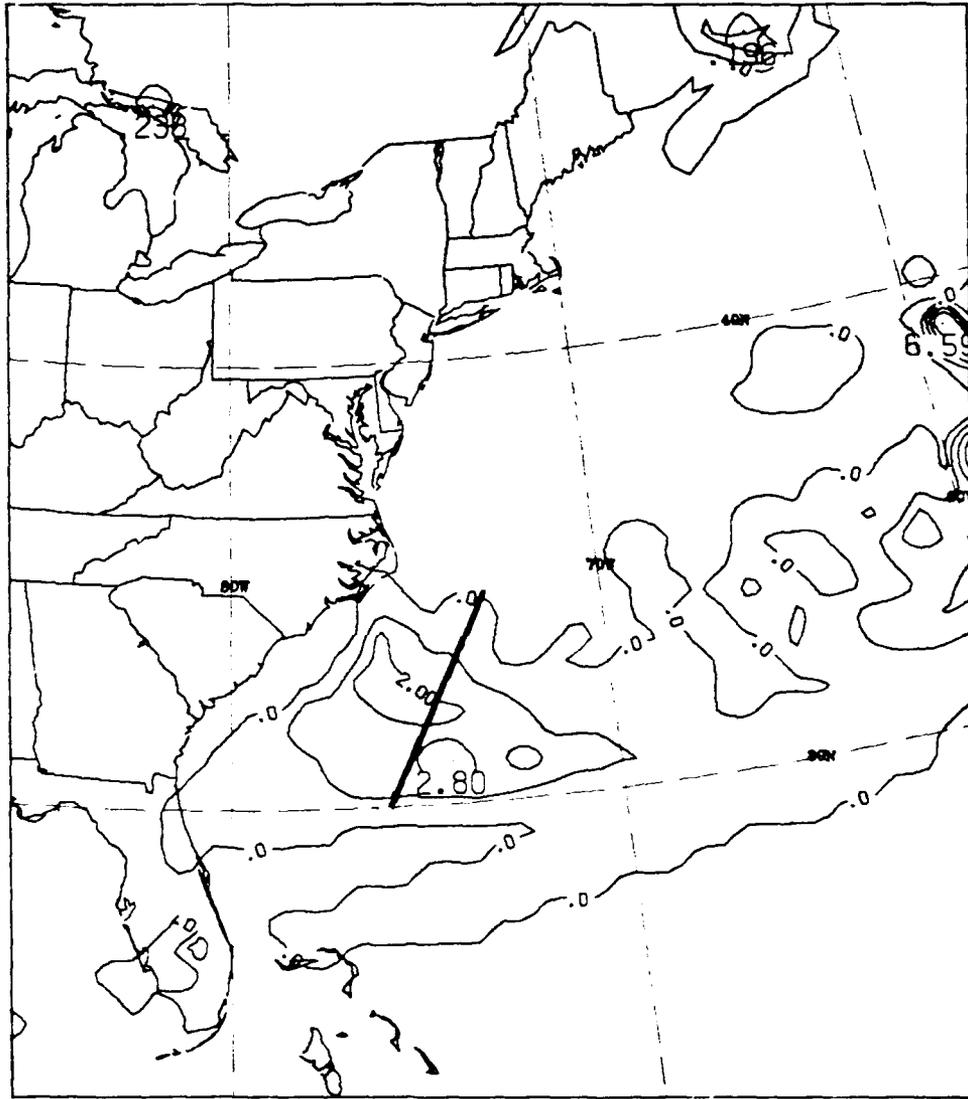
Fig. 14. 12 h forecast of cumulative 12 h convective precipitation (contour interval 1 cm). Solid line indicates cross section location in Figs. 31 & 32.
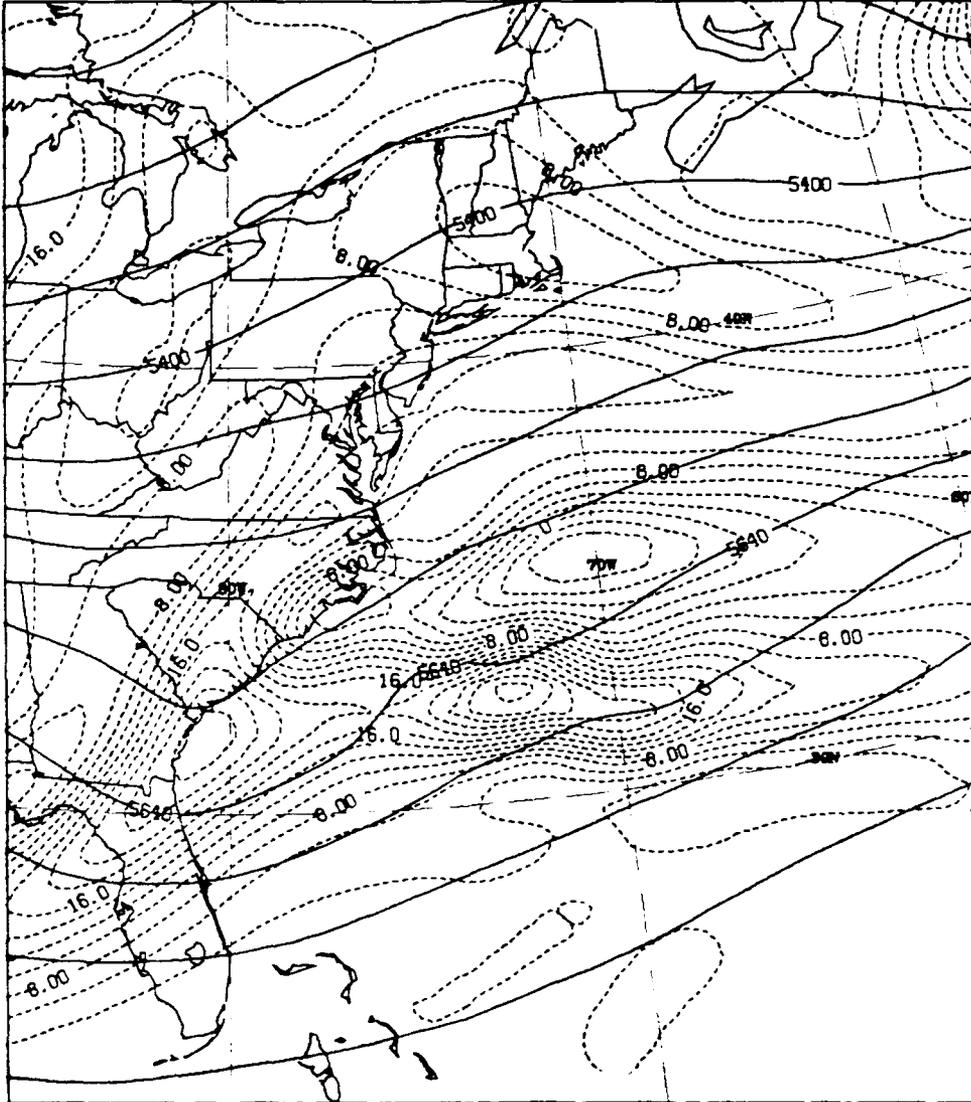
Fig. 15a. 18 h forecast of 500 mb geopotential heights (contour interval 60 m) and absolute vorticity (dashed lines, contour interval 2 s^{-1}) for Simulation 1

51
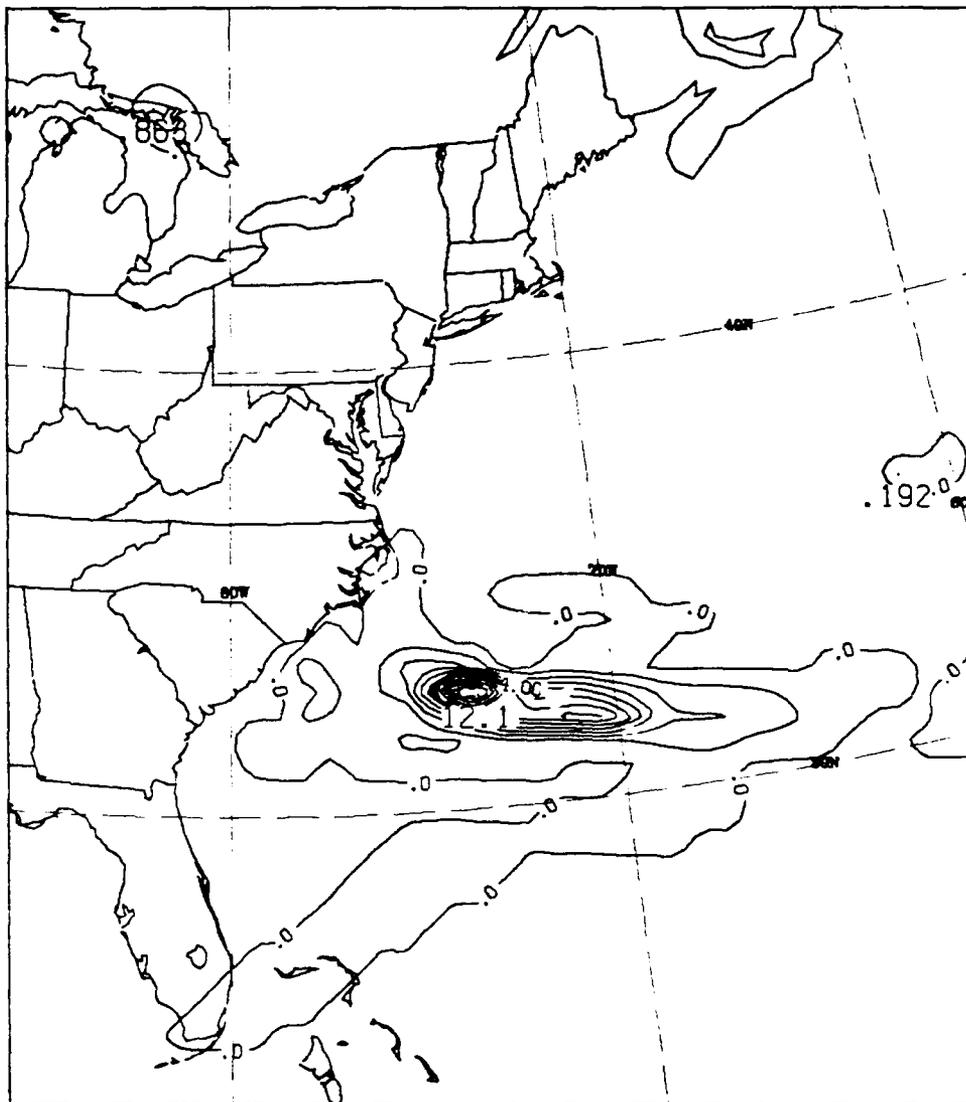
Fig. 15b. 18 h forecast of cumulative 6 h convective precipitation (contour interval 1 cm) for Simulation 1.
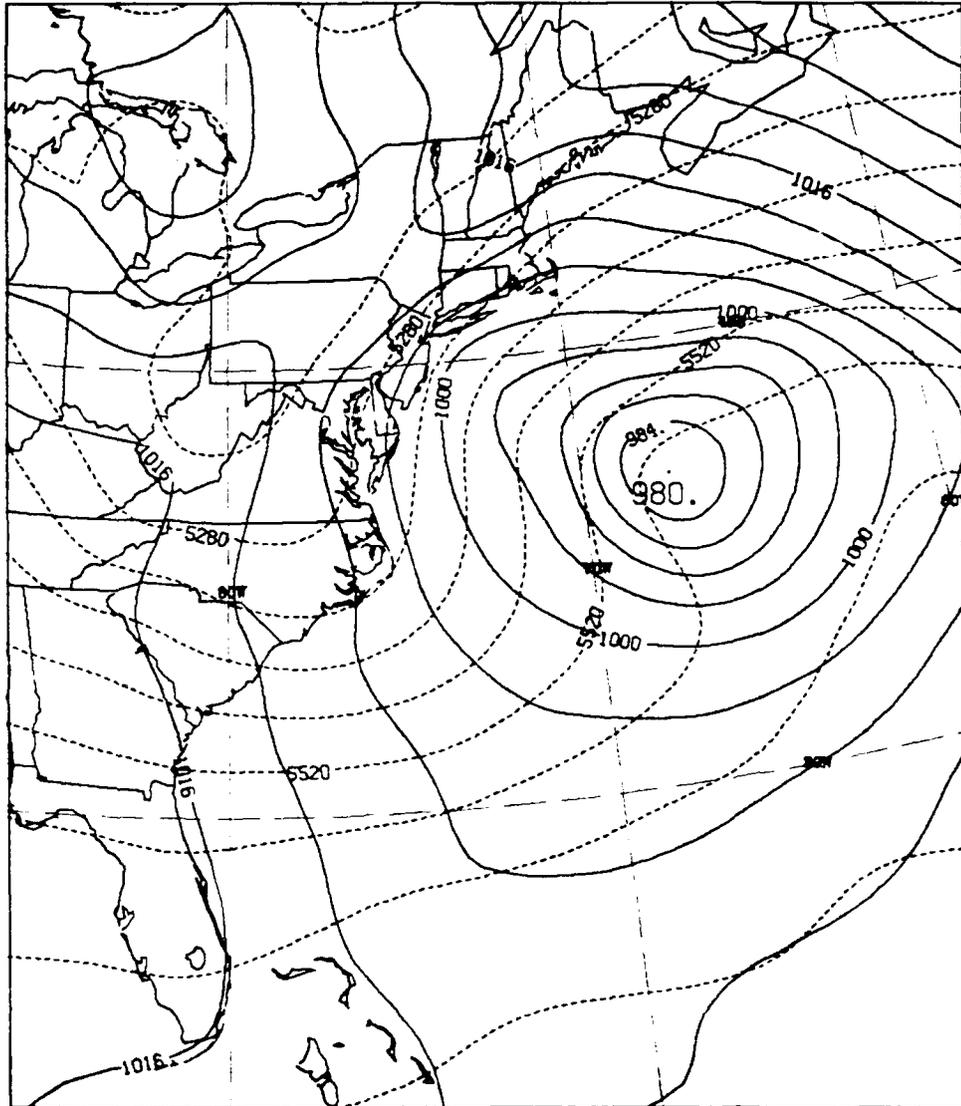
Fig. 16. As in Fig. 11 except for 36 h forecast.
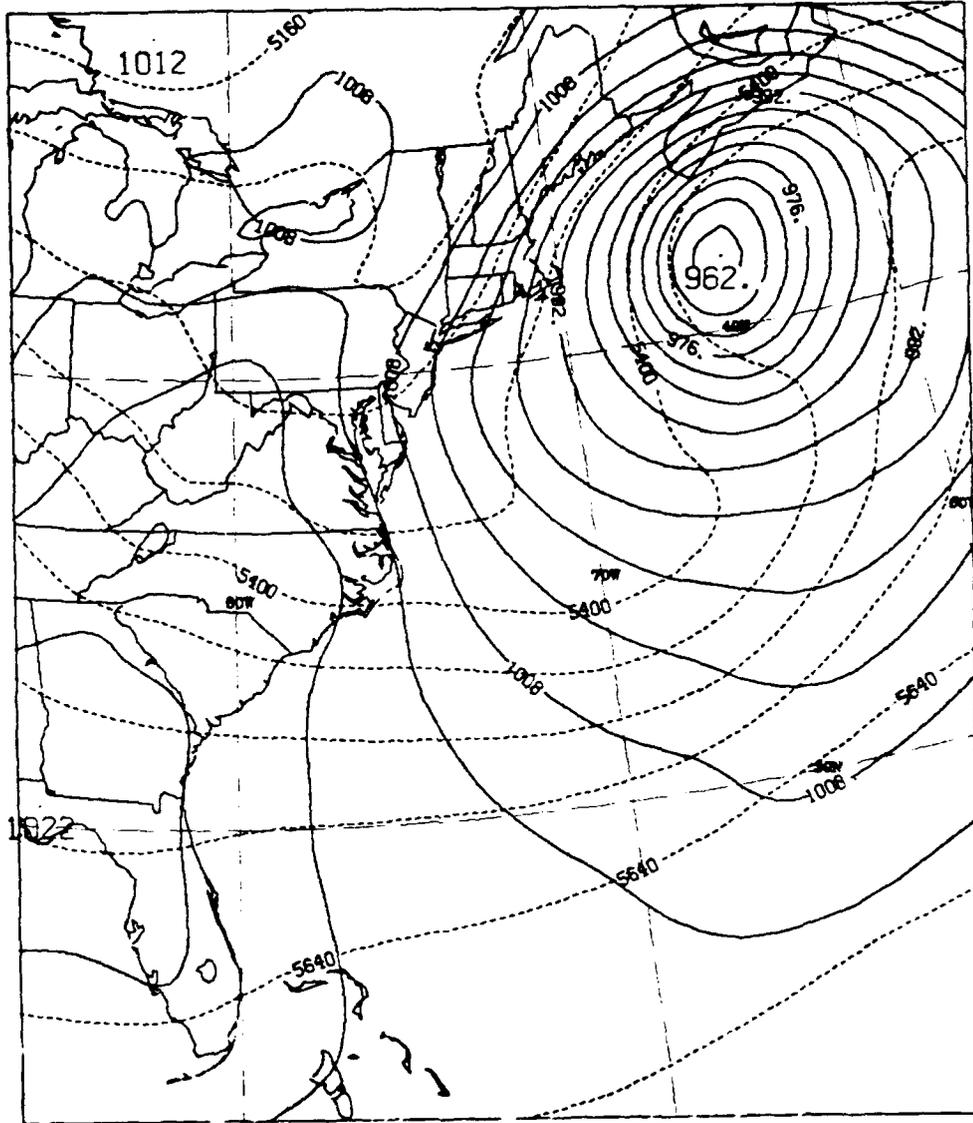
Fig. 17a. As in Fig. 11 except for 48 h forecast for Simulation 1.
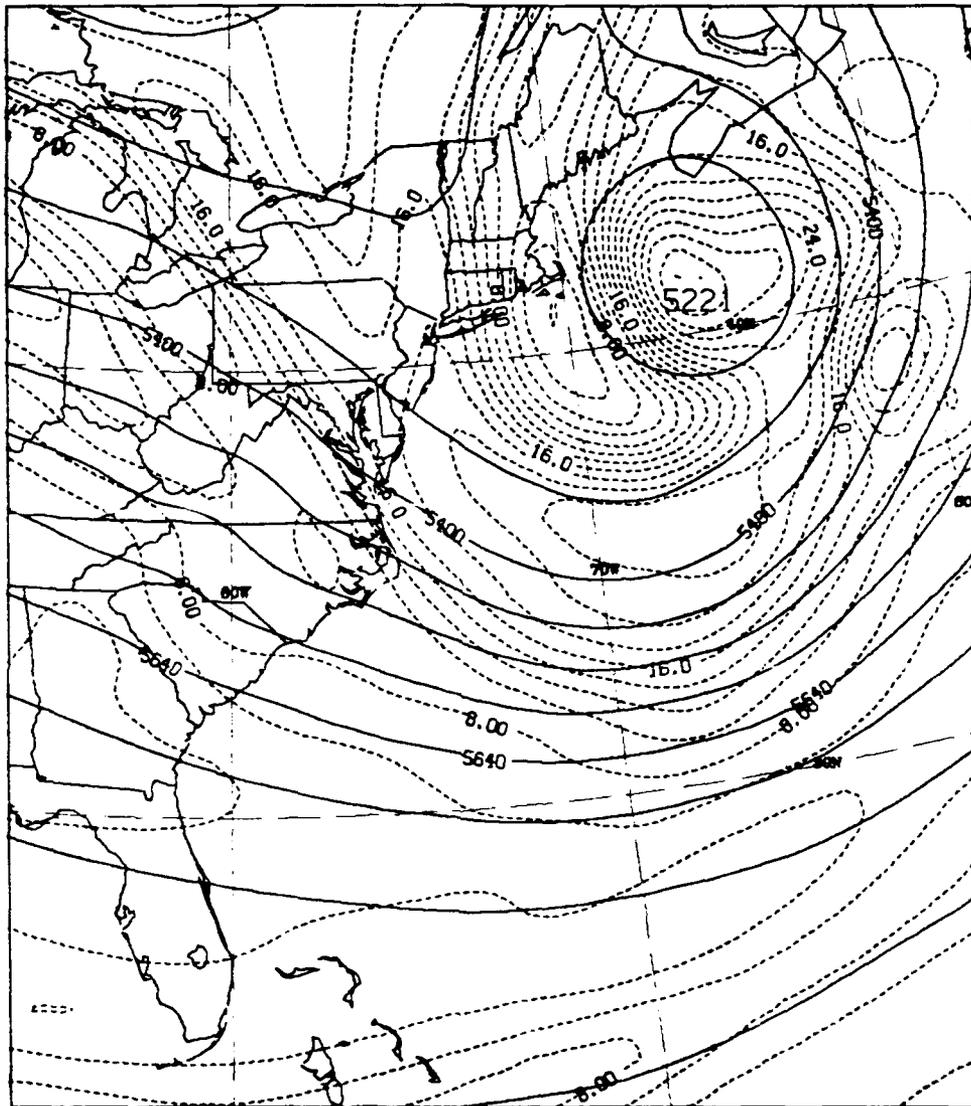
Fig. 17b. As in Fig. 12b except for 48 h forecast for Simulation 1.
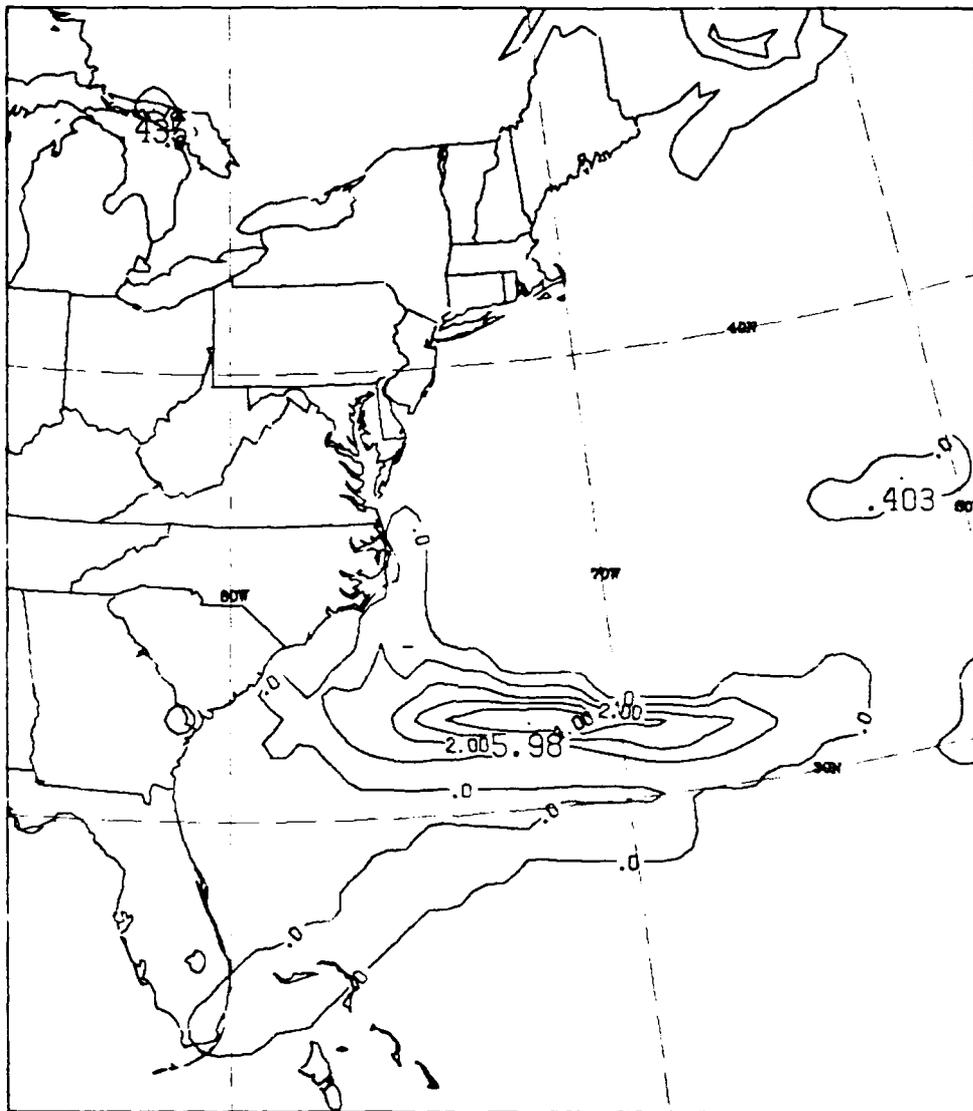
Fig. 18. As in Fig. 15b except for Simulation 2.
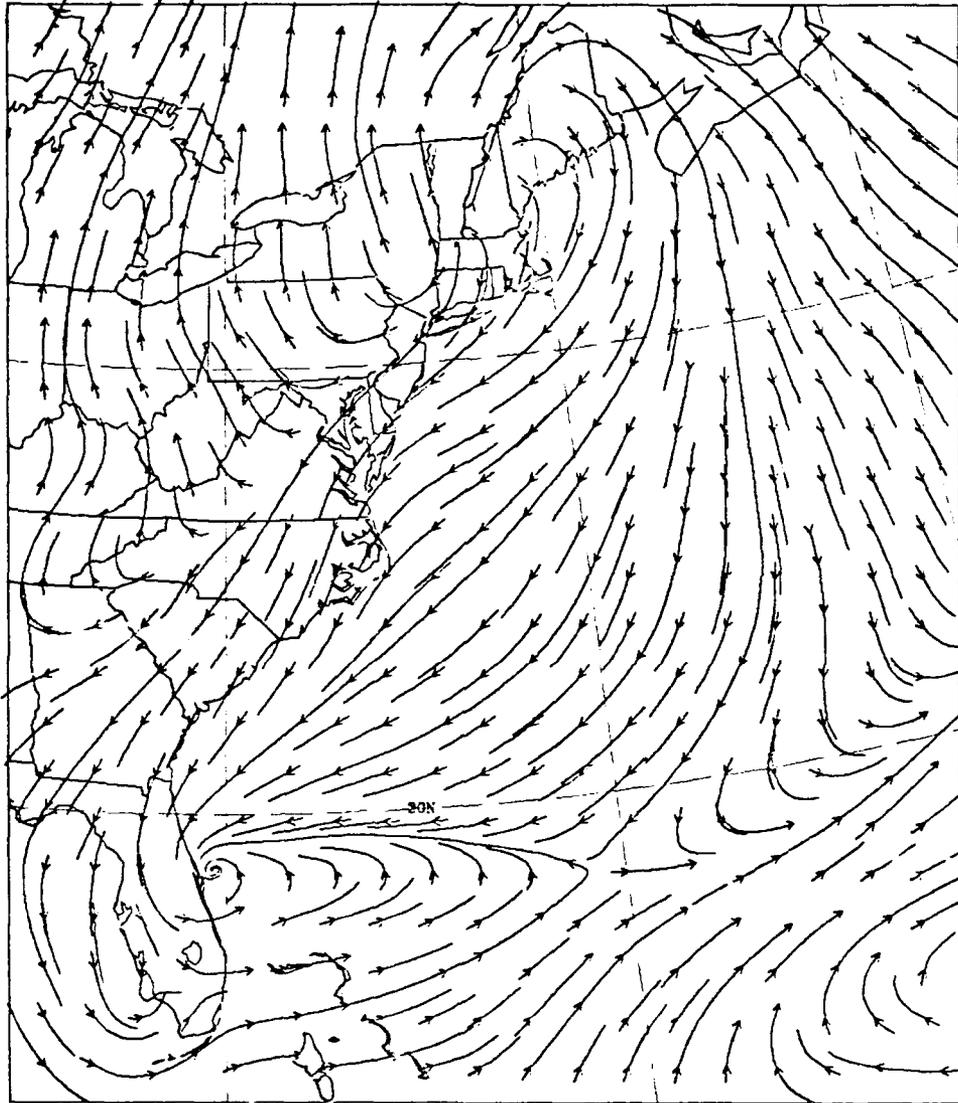
Fig. 19a. As in Fig. 13a except for Simulation 4.
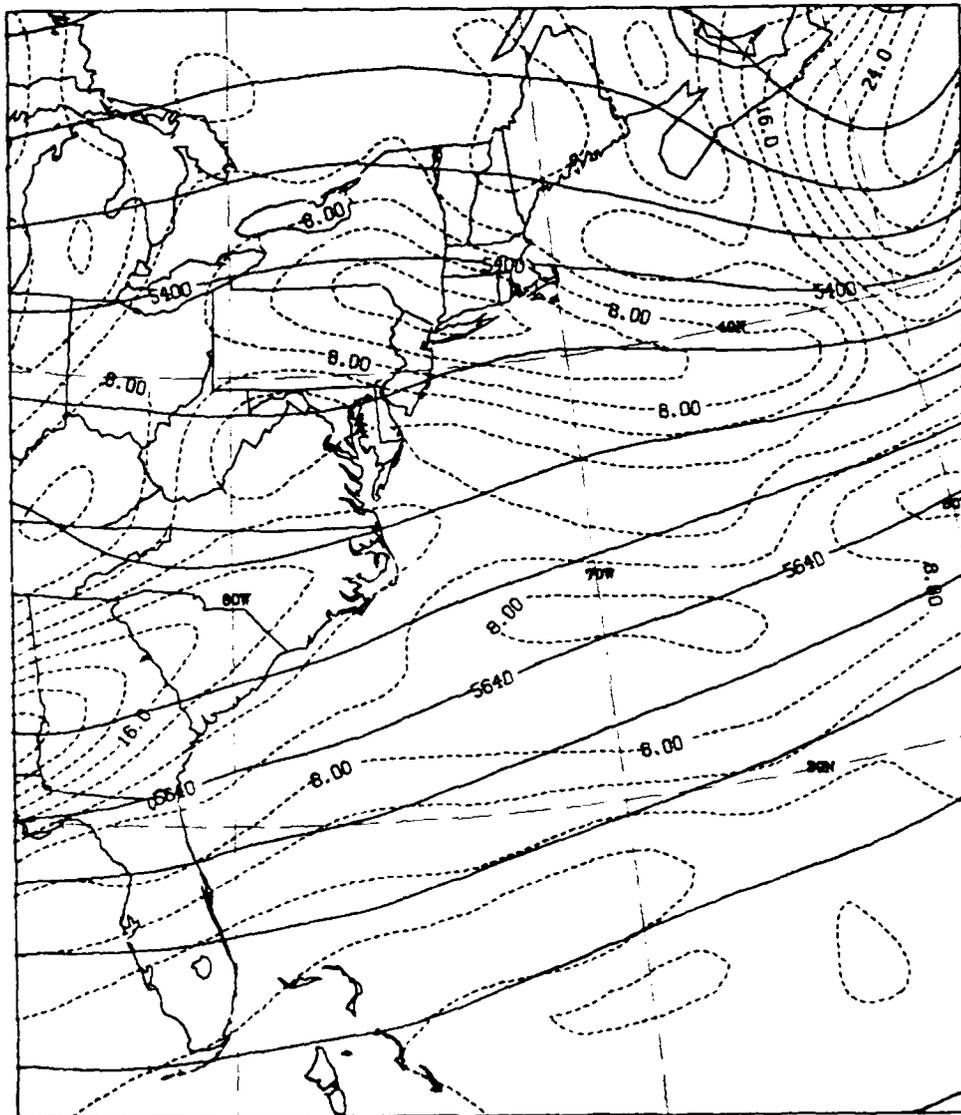
Fig. 19b. As in Fig. 13b except for Simulation 4.
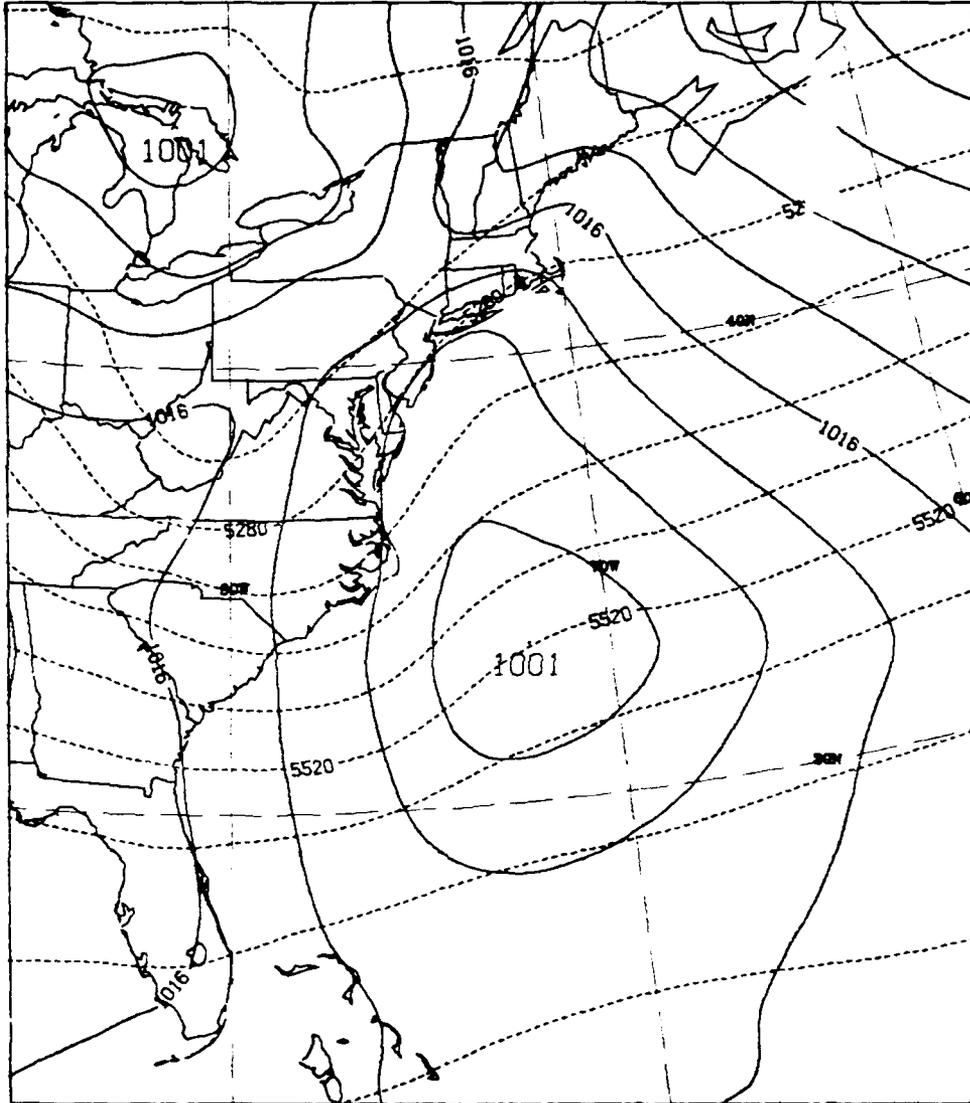
Fig. 20. As in Fig. 11 except for 36 h forecast for Simulation 4.
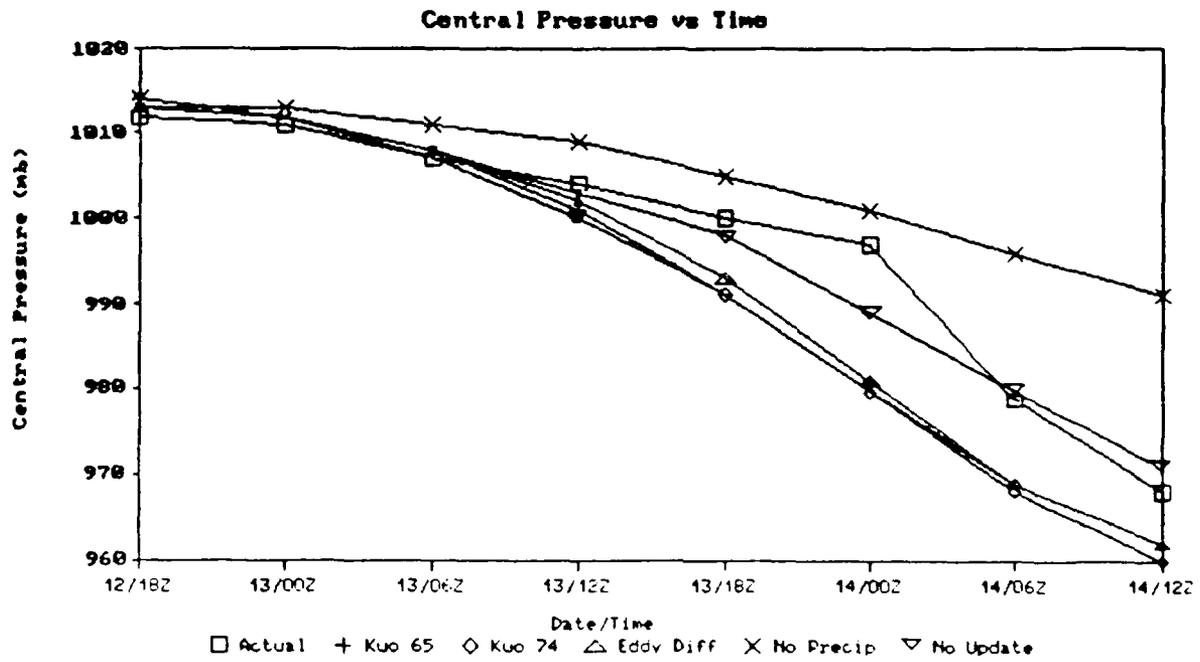
Fig. 21. Observed and forecast central pressures (CP) in mb. Observed CP taken from Chalfant (1989). Forecasts are for Simulations 1 - 5 (see text for explanation on simulations).

60
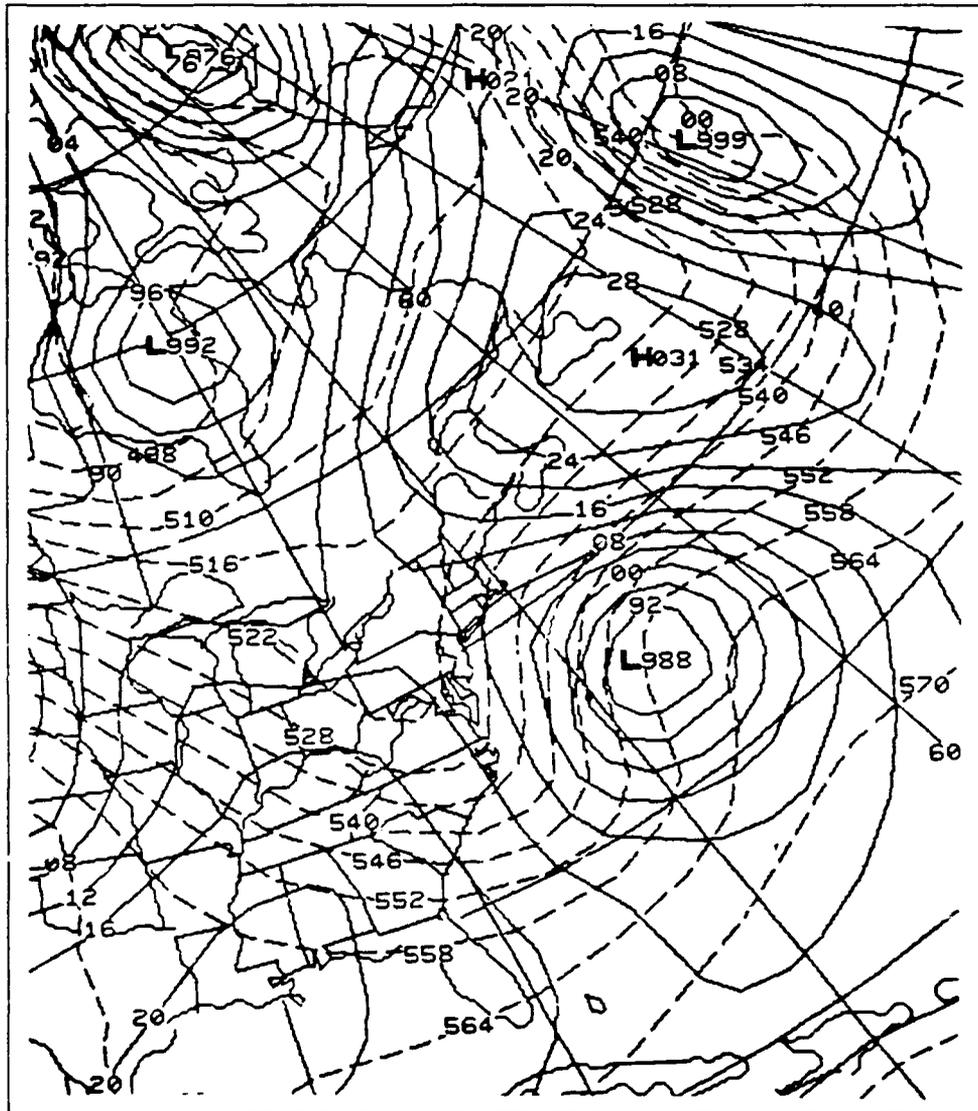
Fig. 22a. NMC Global Spectral Model 36 h forecast of sea level pressure (contour interval 4 mb) and 1000-500 mb thickness (dashed lines, contour interval 60 m).
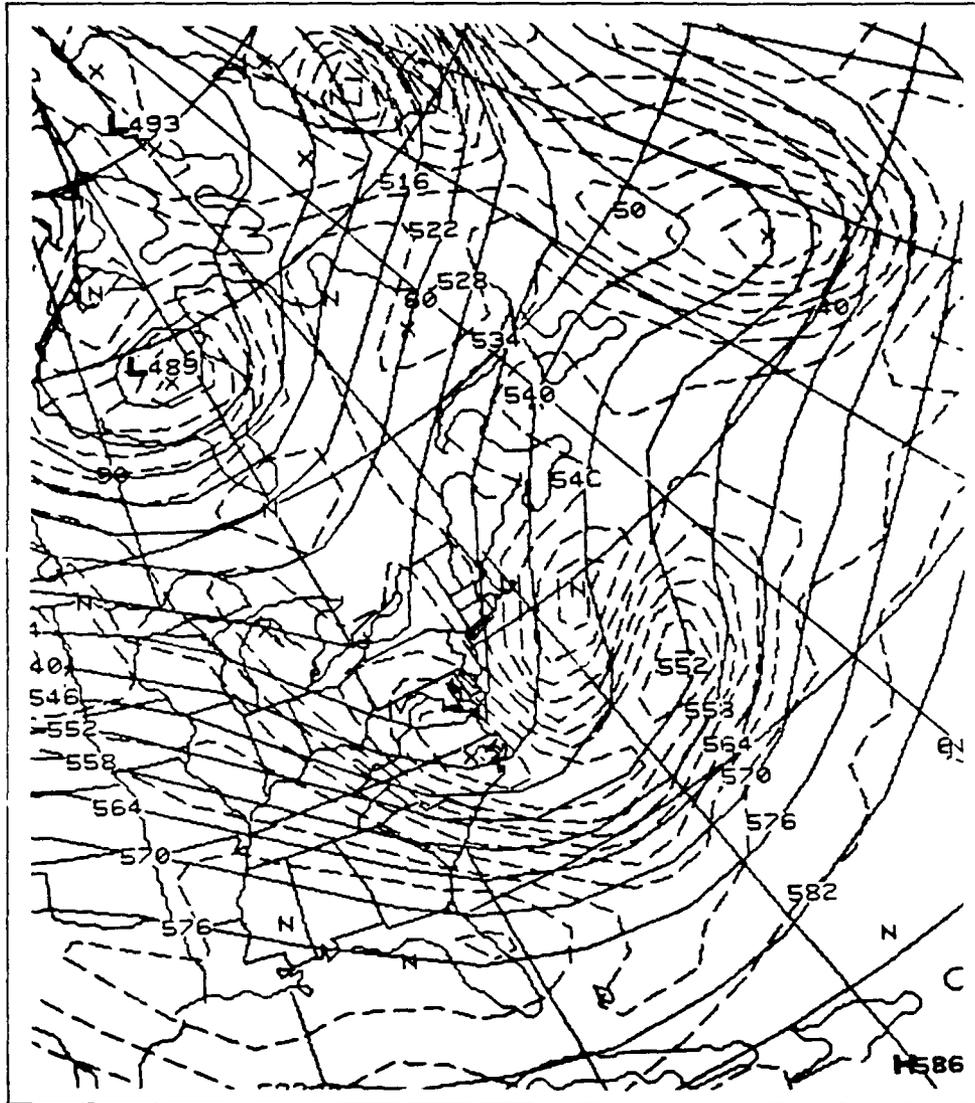
Fig. 22b. NMC Global Spectral Model 36 h forecast of 500 heights (contour interval 60 m) and vorticity (dashed lines, contour interval 2^{-1}).
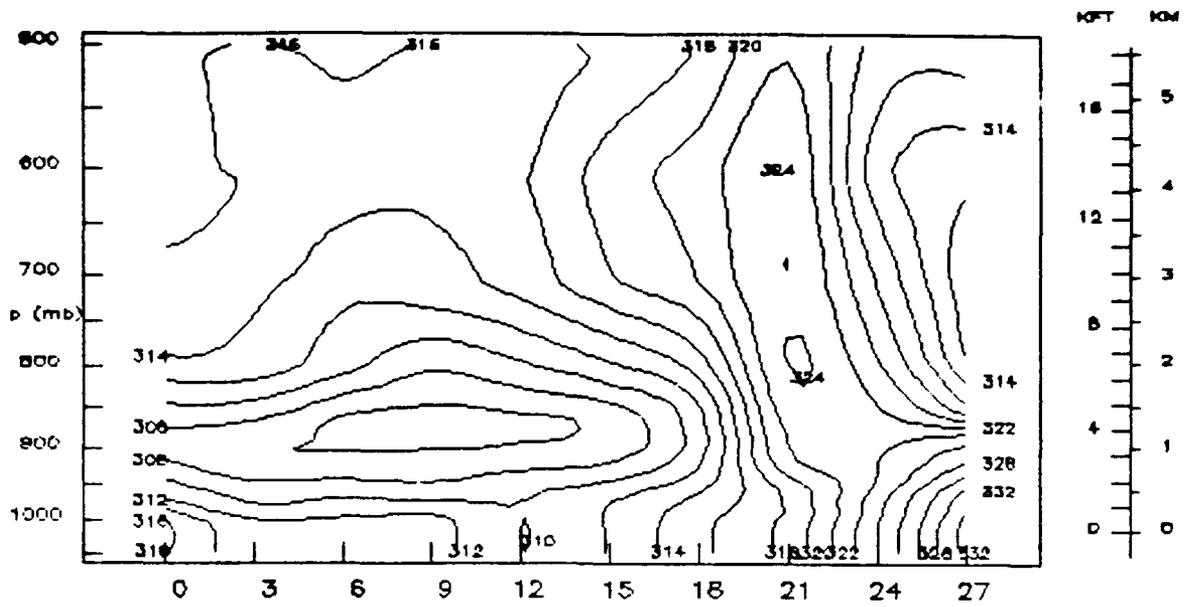
Fig. 23. Vertical time section of equivalent potential temperature (contour interval 2 K) forecast at buoy 40369 (33°N, 70°W) for Simulation 1. Vertical coordinate is pressure in mb. Horizontal coordinate is hours from initial time (1200 UTC 12 December 1988).
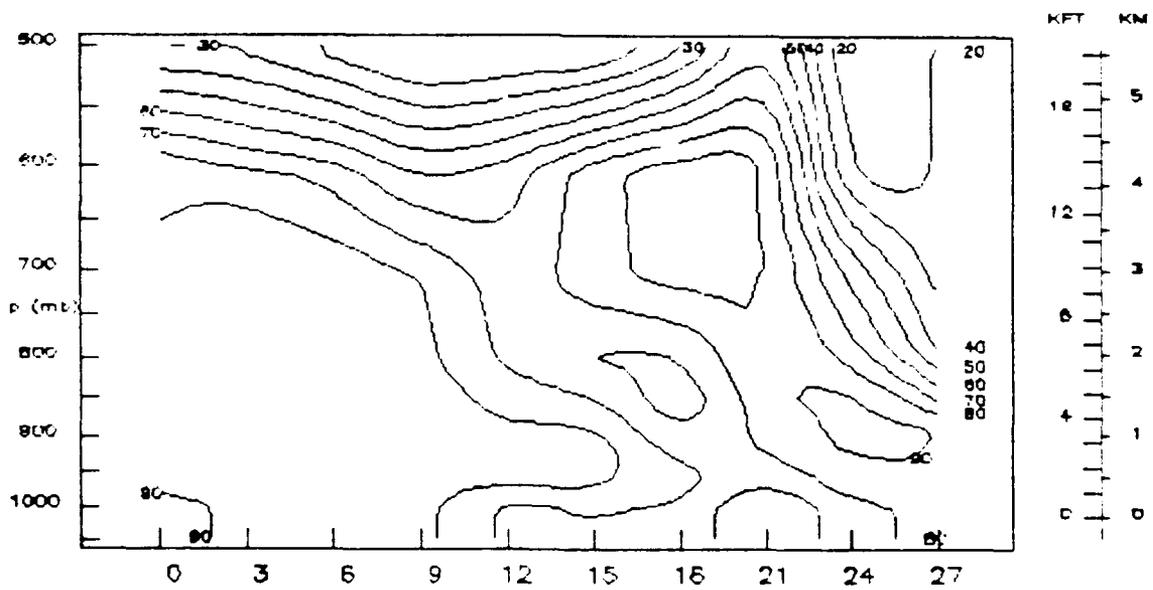
Fig. 24. As in Fig. 23 except for relative humidity (contour interval 10%).

63
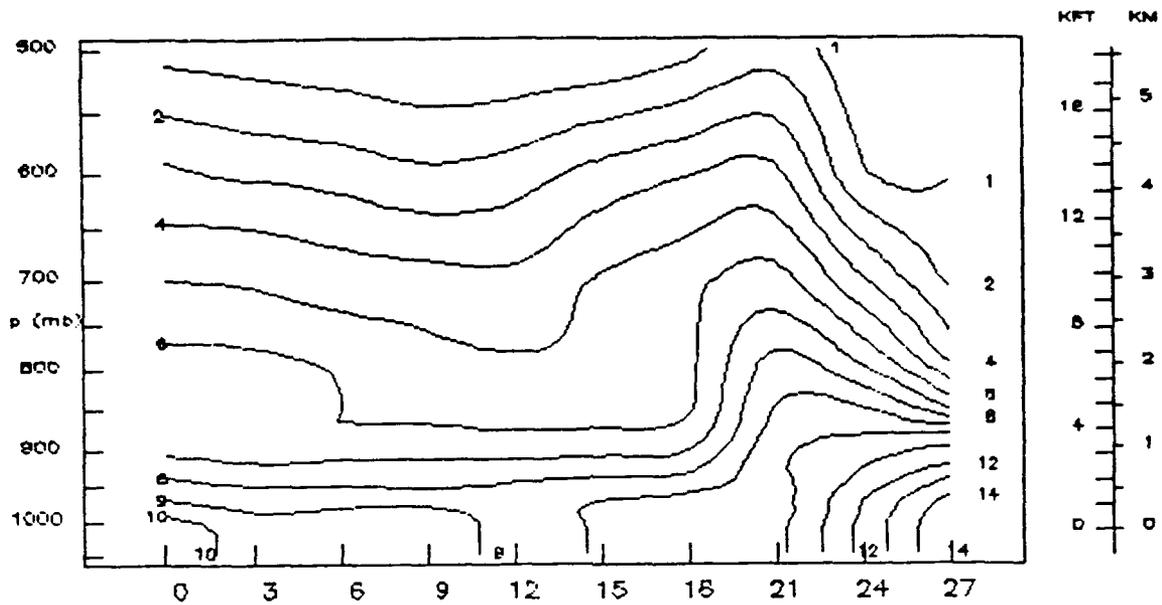
Fig. 25. As in Fig. 23 except for mixing ratio (contour interval 1 g/kg).
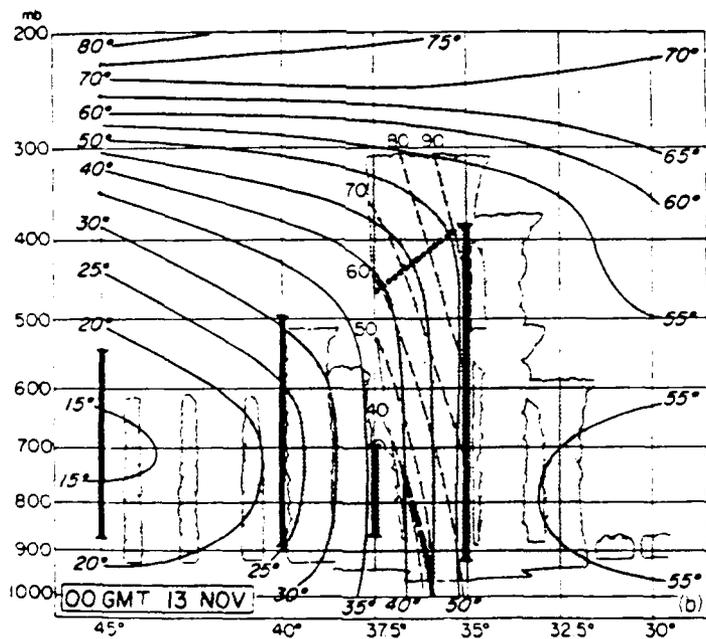
Fig. 26. Vertical cross section of equivalent potential temperature (contour interval 5 °C) and absolute momentum (dashed, contour interval 10 ms^{-1}) along 147.5°W at 0000 UTC 13 November 1981 (from Reed and Albright, 1986). Shading denotes clouds.
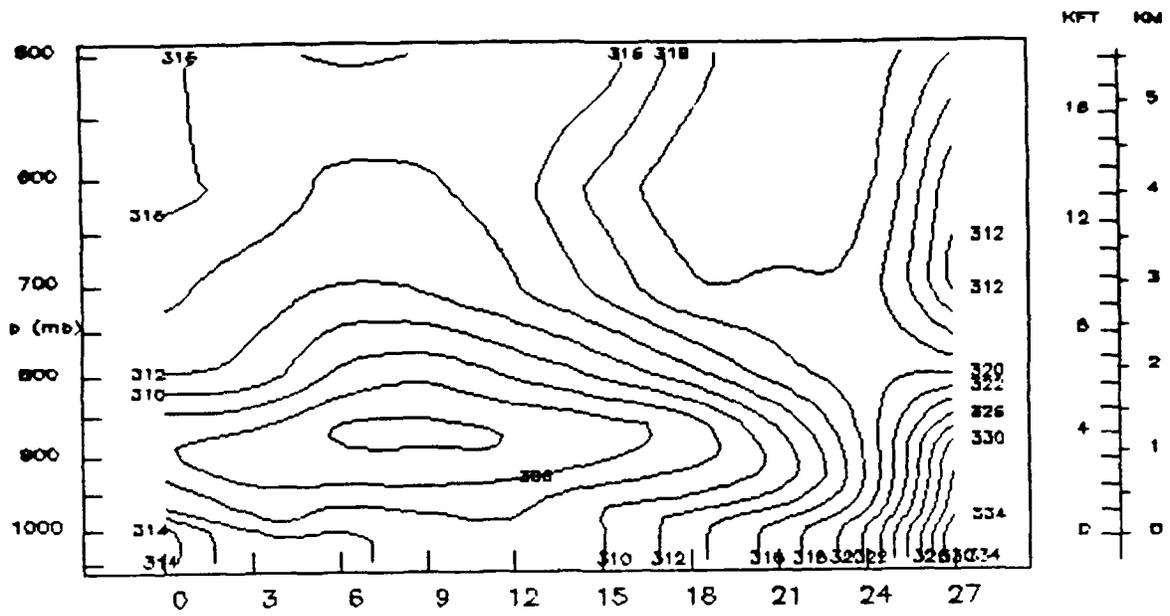
64

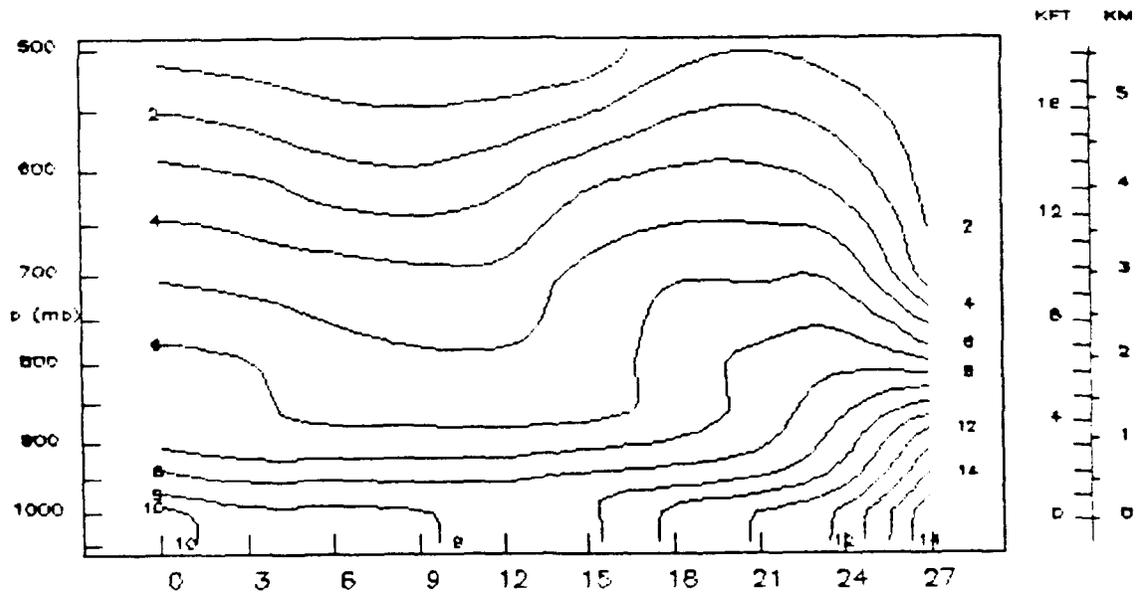Fig. 27. As in Fig. 23 except for Simulation 2.
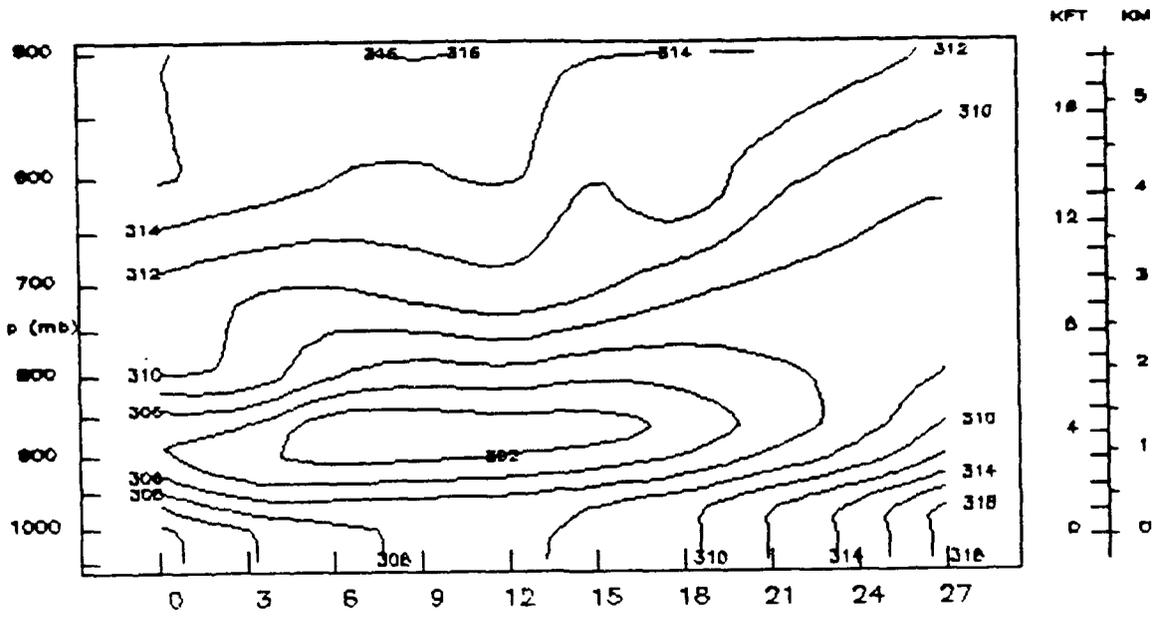

Fig. 28. As in Fig. 25 except for Simulation 2.

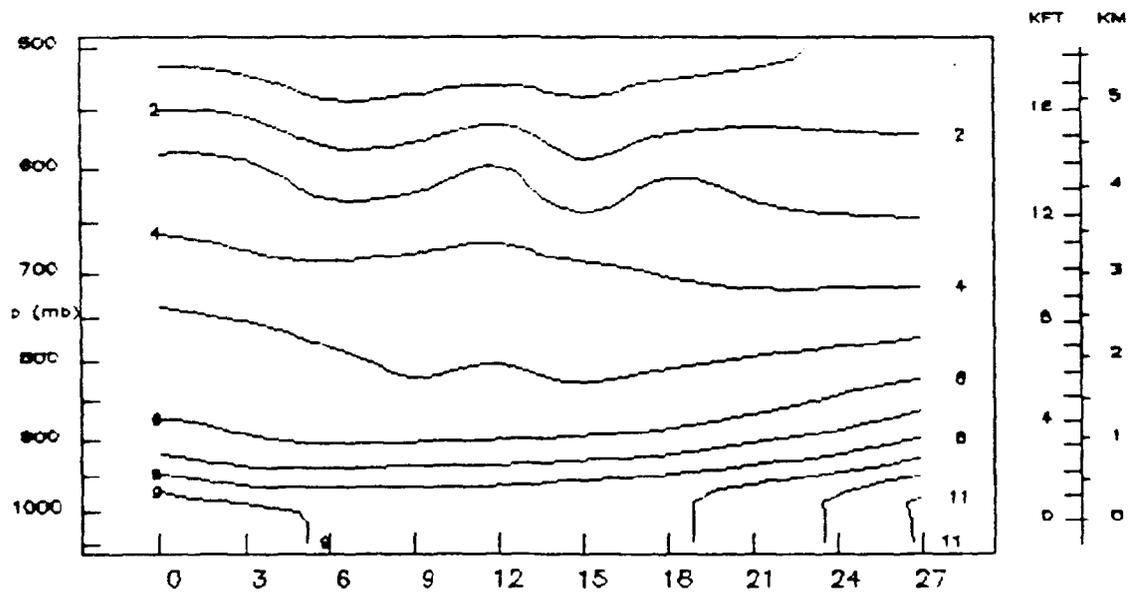Fig. 29. As in Fig. 23 except for Simulation 4.

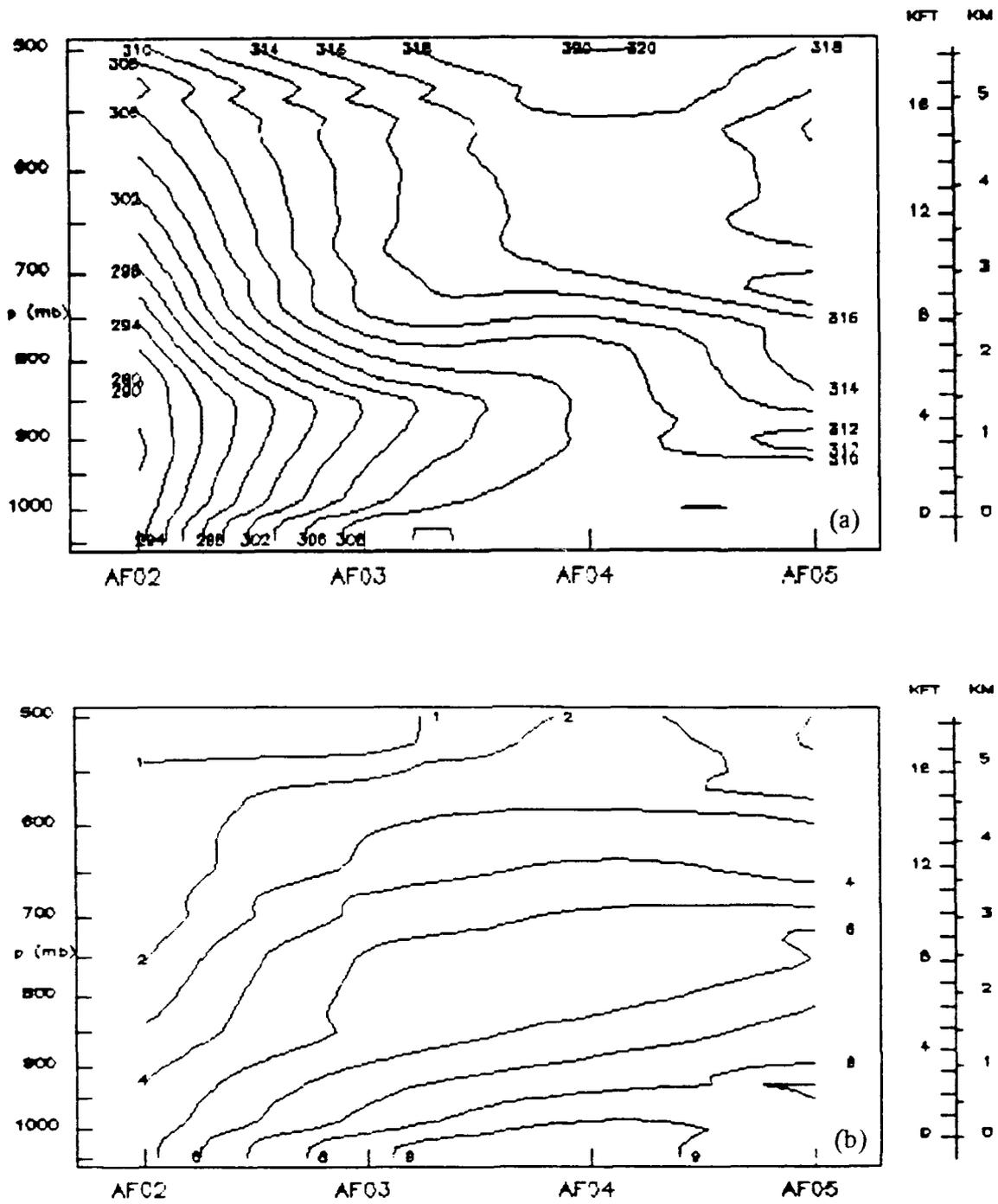Fig. 30. As in Fig. 25 except for Simulation 4.

Fig. 31. Vertical cross section of (a) equivalent potential temperature (contour interval 2 K) and (b) mixing ratio (contour interval 1 g/kg) of four Air Force dropsondes at 0000 UTC 13 December 1988. See Fig. 12 for location of cross section.
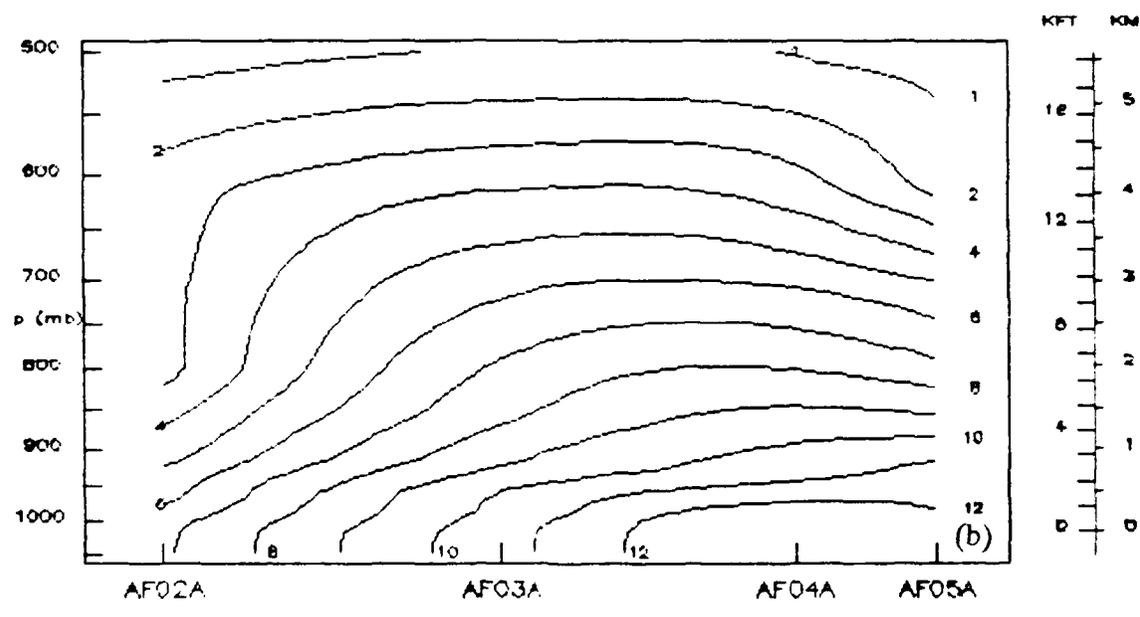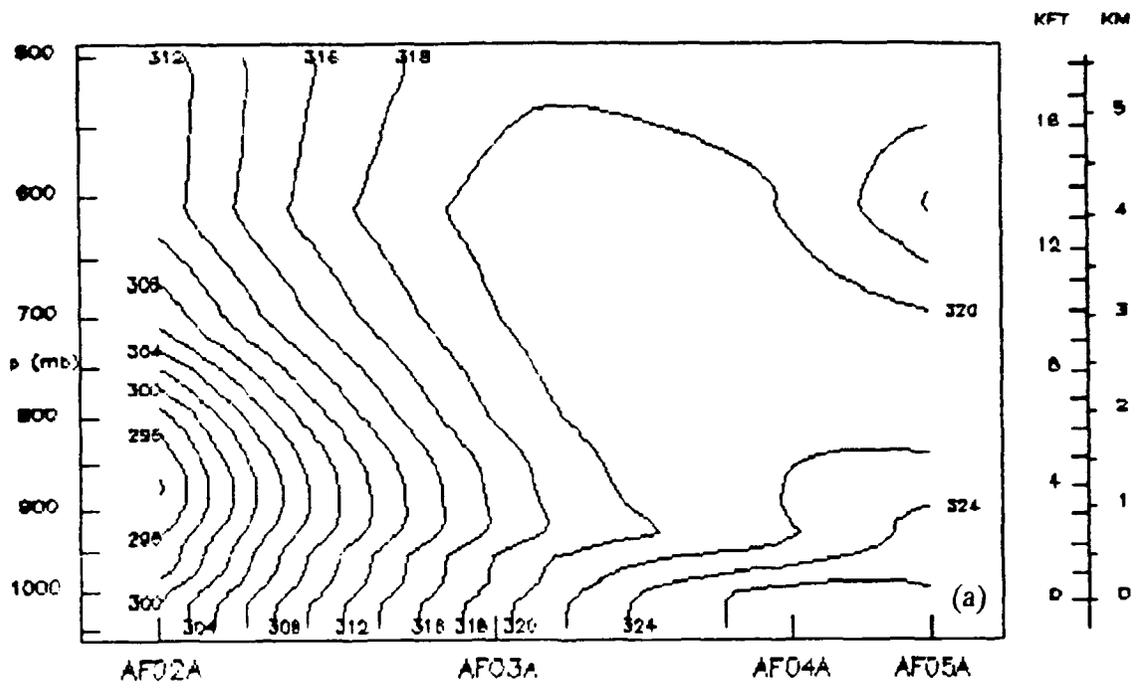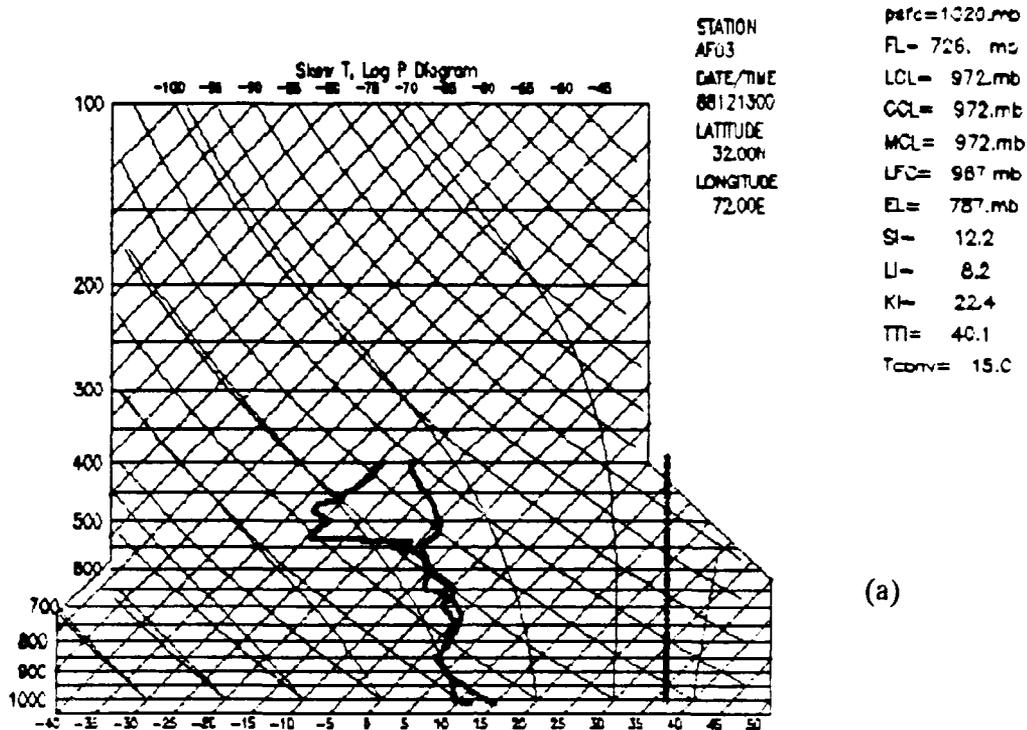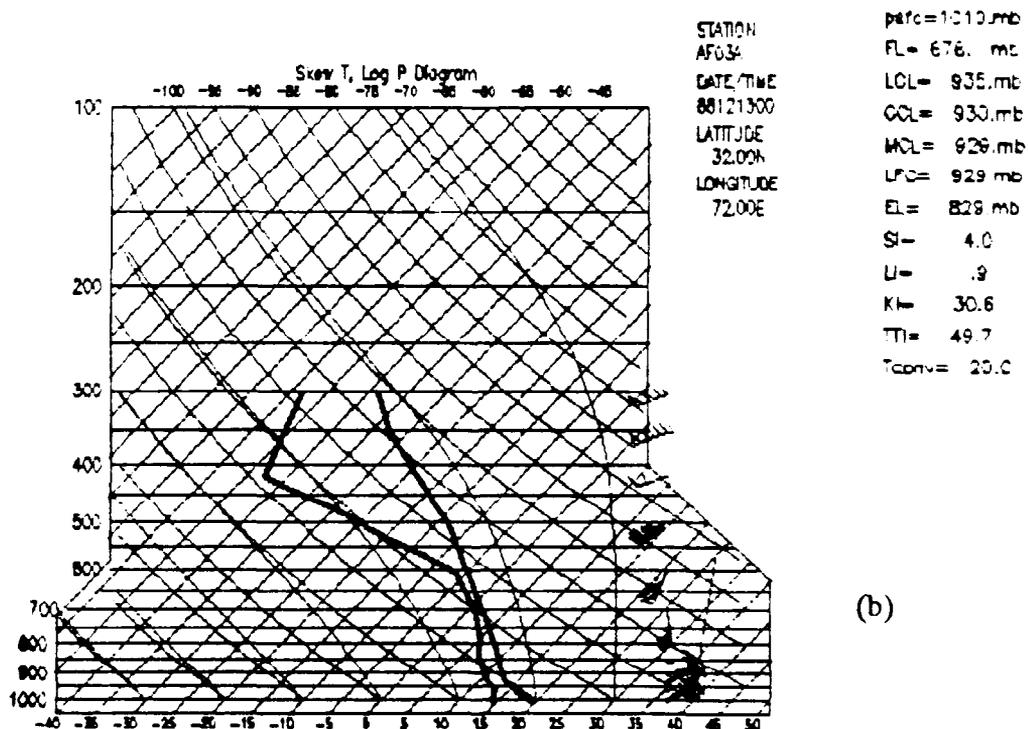
Fig. 32. As in Fig. 31 except for Simulation 1 12 h forecast.

STATION
AF03
DATE/TIME
88121300
LATITUDE
32.00N
LONGITUDE
72.00E

psfc=1020.mb
FL= 726. mc
LCL= 972.mb
CCL= 972.mb
MCL= 972.mb
LFC= 987 mb
EL= 757.mb
SI= 12.2
LI= 8.2
KI= 22.4
TTI= 40.1
Tconv= 15.C

(a)

STATION
AF03A
DATE/TIME
88121300
LATITUDE
32.00N
LONGITUDE
72.00E

psfc=1010.mb
FL= 676. mc
LCL= 935.mb
CCL= 930.mb
MCL= 929.mb
LFC= 929 mb
EL= 829 mb
SI= 4.0
LI= .9
KI= 30.6
TTI= 49.7
Tconv= 20.C

(b)

Fig. 33. Skew-T Log P diagram of (a) Air Force 03 dropsonde and (b) corresponding NORAPS 12 h forecast valid at 0000 UTC 13 December 1988. Temperatures are in °C. Stability indices at right are Showalter Index (SI), Lifted Index (LI), K Index (KI) and Totals Index (TTI).

69
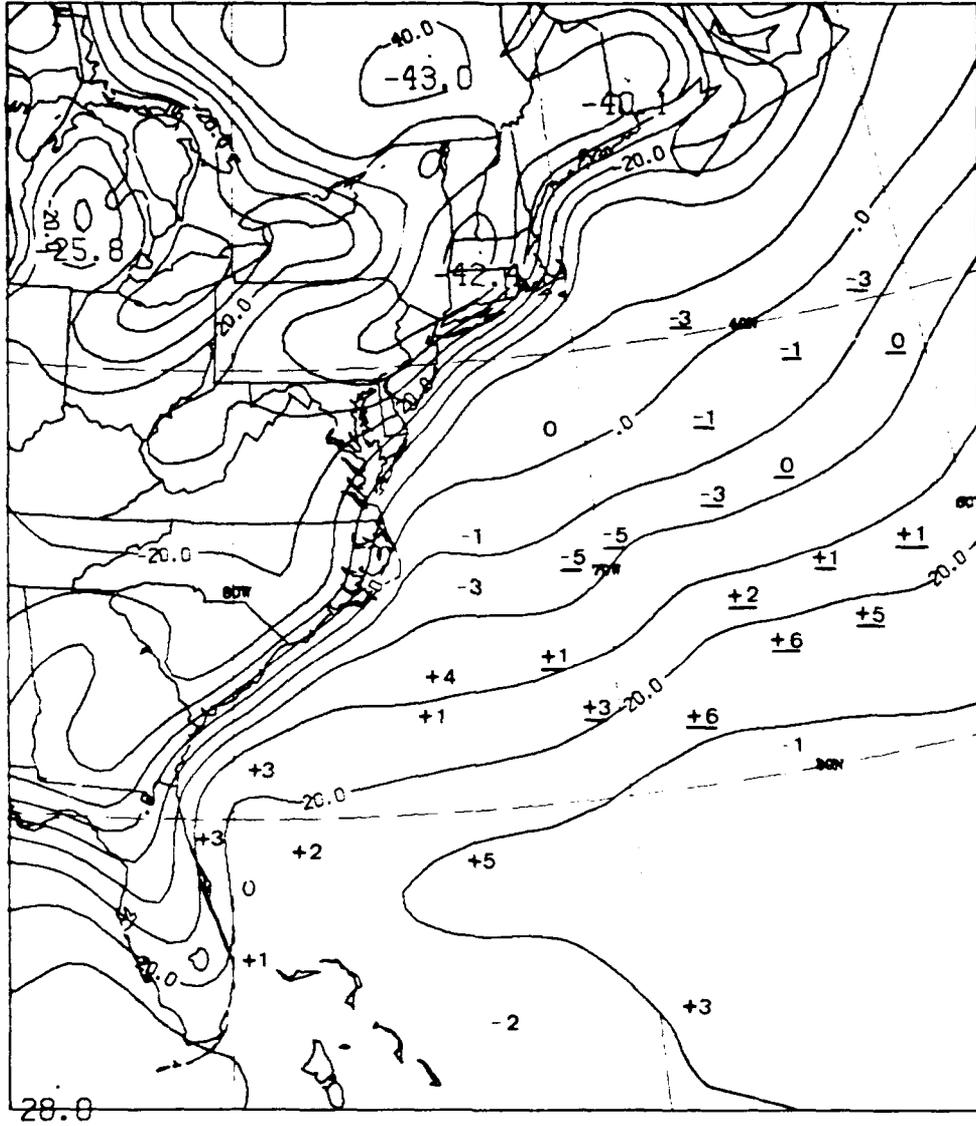
Fig. 34a. 1200 UTC 12 December 1988 analysis of 2 m air temperature by NORAPS. Differences between observed ship and buoy temperatures and the model analyses are also plotted. A positive value indicates that the analysis is warmer than the observation. Underlined numbers indicate ERICA buoys.
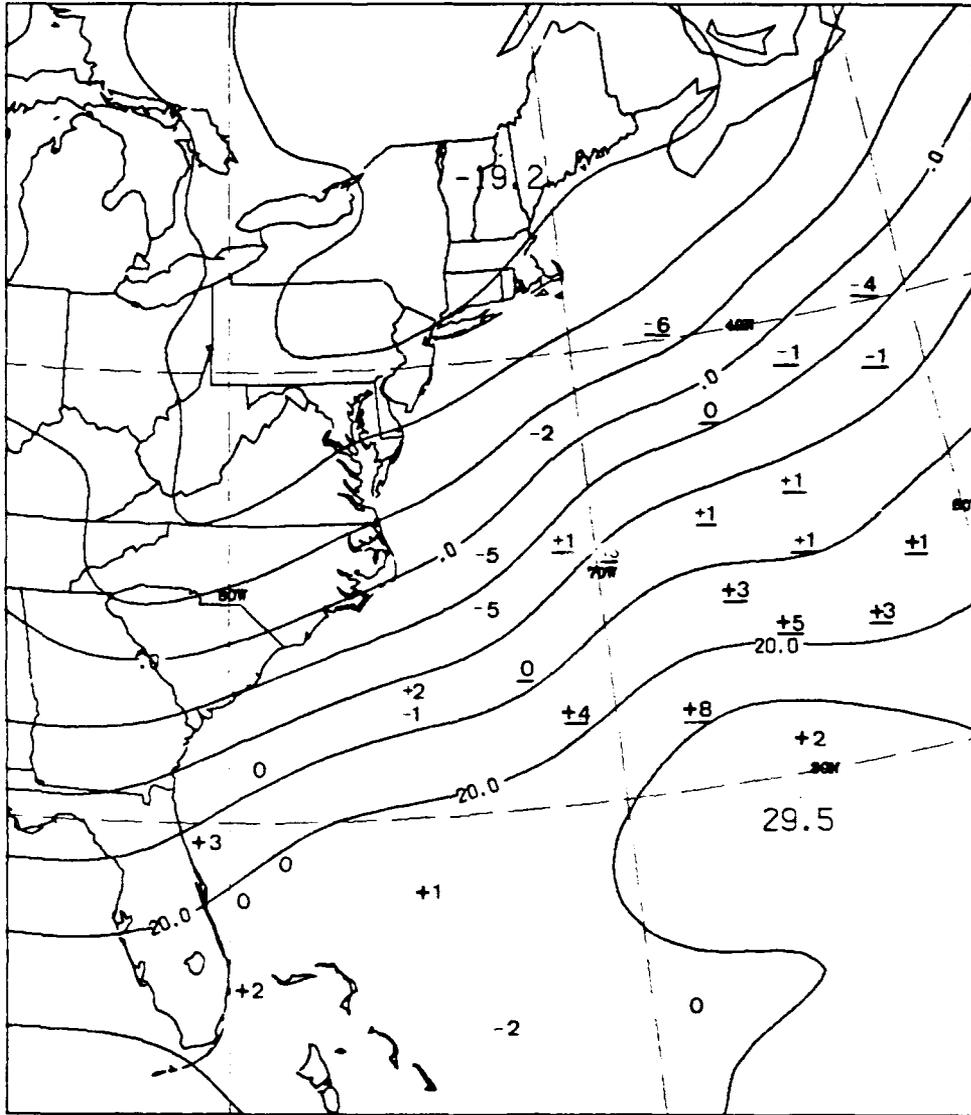
Fig. 34b. As in Fig. 34a except for NOGAPS analysis.

Fig. 35a. 1200 UTC 12 December 1988 analysis of 1000 mb vapor pressure (contour interval 5 mb) by NORAPS.
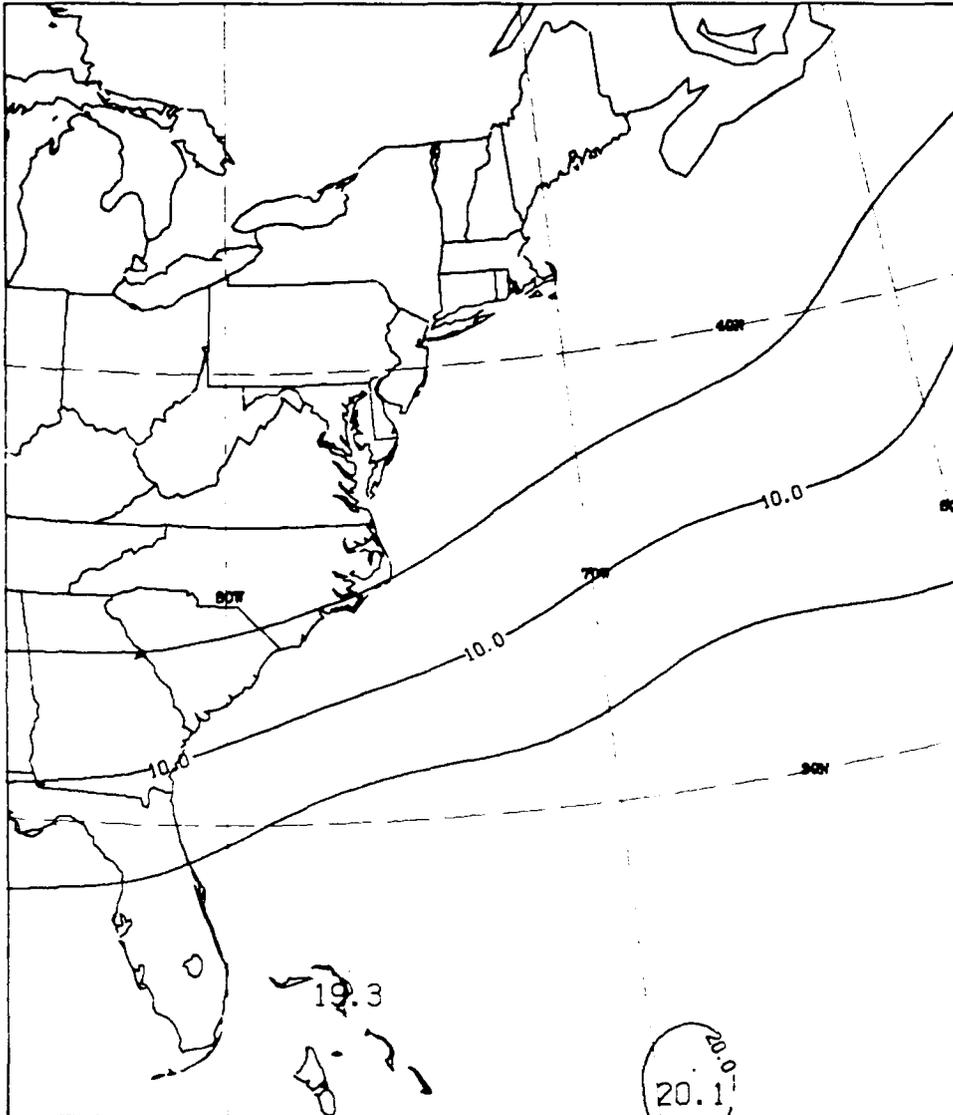
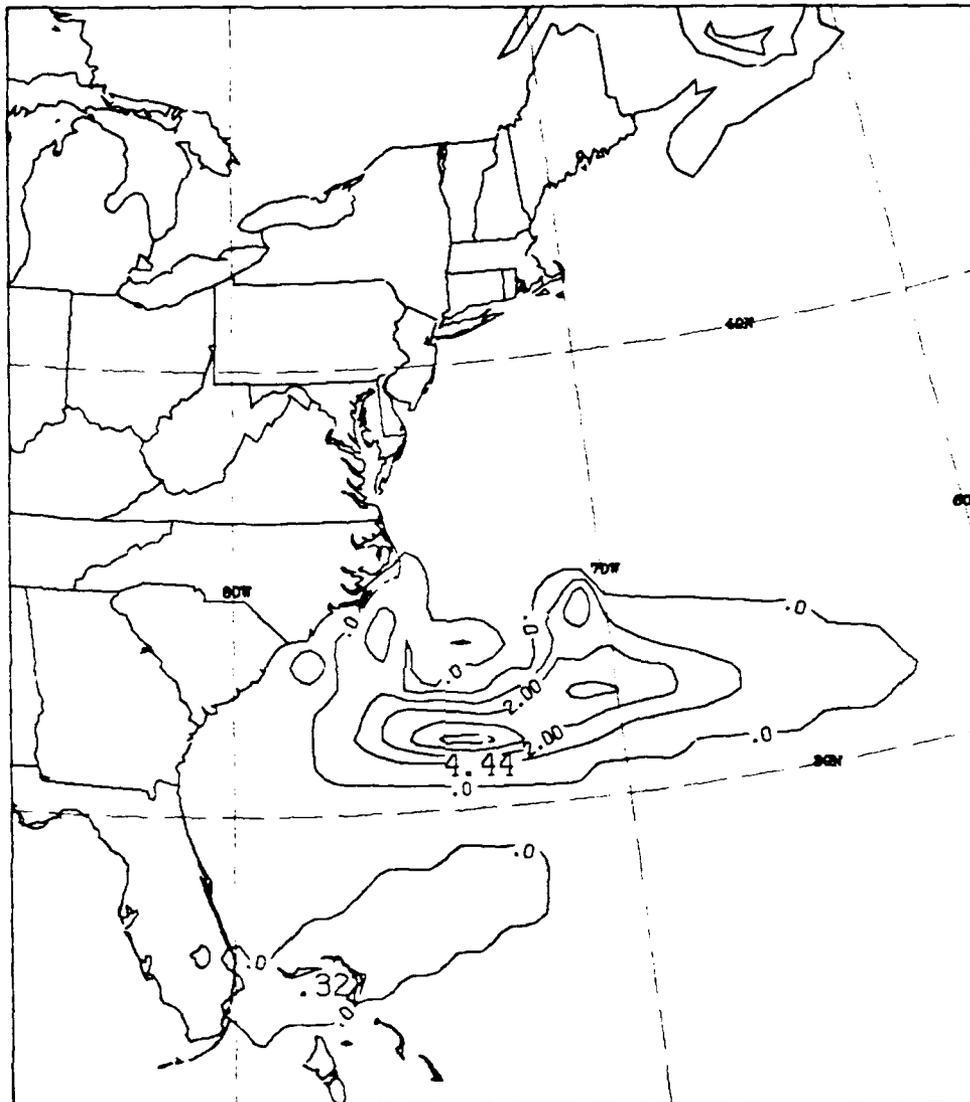Fig. 35b. As in Fig. 35a except for NOGAPS analysis.
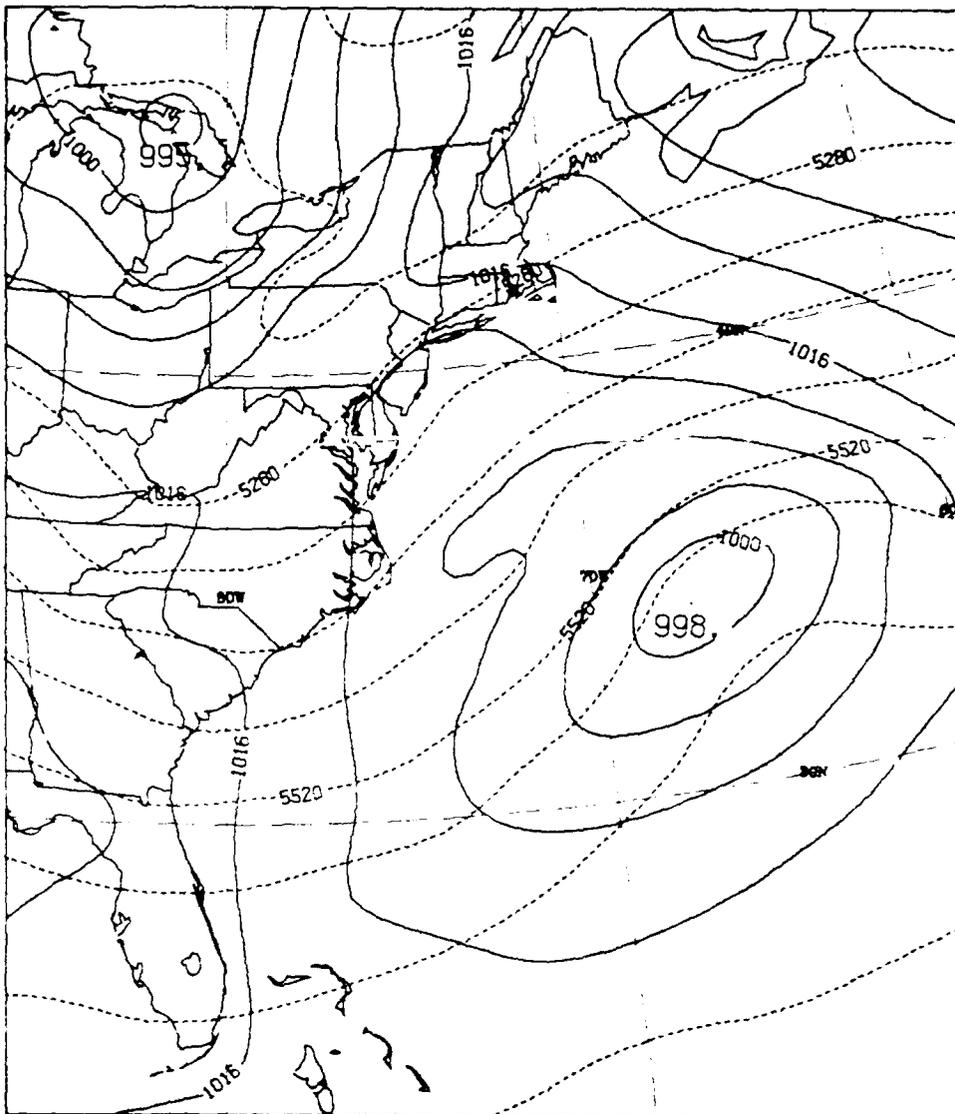
Fig. 36. As in Fig. 15b except for Simulation 5.

Fig. 37. As in Fig. 11 except for 30 h forecast for Simulation 5.
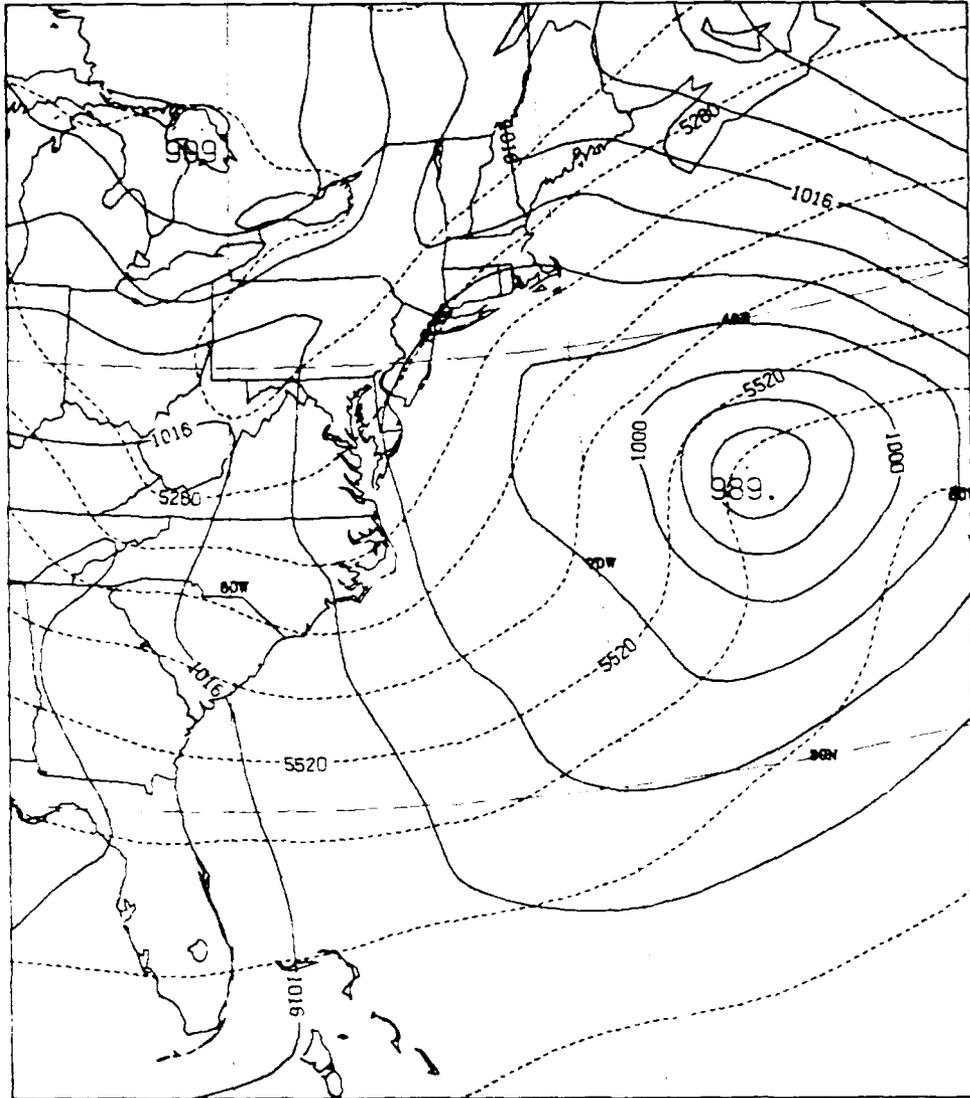
Fig. 38. As in Fig. 11 except for 36 h forecast for Simulation 5.

REFERENCES

Anthes, R. A., Y-H. Kuo and J. R. Gyakum, 1983: Numerical simulations of a case of explosive marine cyclogenesis. *Mon. Wea. Rev.*, 111, 1174-1188.

Arakawa, A., 1971: Design of the UCLA general circulation model, Tech. Rep. No. 7, Dept. Meteor., UCLA, 123 pp. [NTIS N73-21508].

-----, and V. R. Lamb, 1977: Computational design of the UCLA general circulation model. *Methods in Computational Physics*, Vol. 17, Academic Press, 173-265.

-----, and W. H. Schubert, 1974: Interaction of a cumulus cloud ensemble with the large scale environment, Part I. *J. Atmos. Sci.*, 31, 674-701.

Blackadar, A. K., 1977: High resolution models of the planetary boundary layer. *Advances in Environmental Science and Engineering*, Vol. 1, Gordon and Breach, 50-85.

Chalfant, A. E., 1989: Dynamics of an ERICA cyclone. Naval Postgraduate School M.S. Thesis, 54 pp.

Danard, M. B., 1985: On the sensitivity of predictions of maritime cyclogenesis to convective precipitation and sea temperature. *Atmos.-Ocean*, 24, 52-72.

Deardorff, J. W., 1972: Parameterization of the planetary boundary layer for use in general circulation models. *Mon. wea. rev.*, 100, 93-106.

Hadlock, R., 1988: *Experiment on Rapid Intensification of Cyclones over the Atlantic (ERICA) Field Operations Plan*. ERICA Project Office, Battelle Ocean Sciences, Richland, Washington, 280pp.

Hartnett, E., G. Forbes and R. Hadlock, 1989: *Experiment on Rapid Intensification of Cyclones over the Atlantic (ERICA) Field Phase Summary*. Department of Physics and Atmospheric Science, Drexel University, Philadelphia, PA, 300pp.

Hodur, R.M., 1987: Evaluation of a regional model with an update cycle. *Mon. Wea. Rev.*, 115, 2707-2718.

Johnson, D. R., and W. K. Downey, 1976: The absolute angular momentum budget of an extratropical cyclone: quasi-lagrangian diagnostics 3. *Mon. Wea. Rev.*, 104, 3-14.

Kocin, P. J., and L. W. Uccellini, 1989: *Snowstorms Along the Northeastern Coast of the United States: 1955 to 1985*. Meteor. Monographs, (in press).

Krishnamurti, T. N., 1968: A study of a developing wave cyclone. *Mon. Wea. Rev.*, 96, 208-217.

Kuo, H. L., 1965: On formation and intensification of tropical cyclones through latent heat release by cumulus convection. *J. Atmos. Sci.*, **22**, 40-63.

-----, 1974: Further studies of the parameterization of the influence of cumulus convection on the large-scale flow. *J. Atmos. Sci.*, **31**, 1232-1240.

Kuo, Y-H., and S. Low-Nam, 1990: Prediction of nine explosive cyclones over the western Atlantic Ocean with a regional model. *Mon. Wea. Rev.*, **118**, 3-25.

Leslie, L. M., G. J. Holland, and A. H. Lynch, 1987: Australian east-coast cyclones. Part II: Numerical Modeling Study. *Mon. Wea. Rev.*, **115**, 3037-3053.

Liou, C.-S. E., and R. L. Elsberry, 1987: Heat budgets of analyses and forecasts of an explosively deepening maritime cyclone. *Mon. Wea. Rev.*, **115**, 1809-1824.

-----, C. H. Wash, S. M. Heikkinen, and R. L. Elsberry, 1990: Numerical studies of cyclogenesis events during the second intensive observation period (IOP-2) of GALE. *Mon. Wea. Rev.*, **118**, 218-233.

Louis, J. F., M. Tiedtke, and J. F. Geleyn, 1982: A short history of the operational PBL - parameterization at ECMWF. *ECMWF's Workshop on Planetary Boundary Parameterization, 25-27 November 1981*, 59-79.

Madala, R. V., 1982: *Finite Difference Techniques for Vectorized Fluid Dynamic Calculation*. Springer-Verlag, 226 pp.

Mullen, S. L., and D. P. Baumhefner, 1988: Sensitivity of numerical simulations of explosive oceanic cyclogenesis to changes in physical parameterizations. *Mon. Wea. Rev.*, **116**, 2289-2329.

Reed, R. J. and M. D. Albright, 1986: A case study of explosive cyclogenesis in the eastern Pacific. *Mon. Wea. Rev.*, **114**, 2297-2319.

Robert, A. J., 1966: The investigation of a low order spectral form of the primitive meteorological equations. *J. Meteor. Soc. Japan*, Ser. 2, **44**, 237-245.

Robertson, F. R. and P. J. Smith, 1983: The impact of model moist processes on the energetics of extratropical cyclones. *Mon. Wea. Rev.*, **111**, 723-744.

Rogers, E. and L. F. Bosart, 1986: An investigation of explosively deepening oceanic cyclones. *Mon. Wea. Rev.*, **114**, 702-718.

Sanders, F., 1987: Skill of NMC operational dynamic models in prediction of explosive cyclogenesis. *Weather and Forecasting*, **2**, 322-336.

-----, and J. R. Gyakum, 1980: Synoptic-dynamic climatology of the "bomb". *Mon. Wea. Rev.*, **108**, 1589-1606.

Sasamori, T., 1968: The radiative cooling calculation for application to general circulation experiments. *J. Atmos. Sci.*, **7**, 721-729.

Uccellini, L. W., 1986: The possible influence of upstream upper-level baroclinic processes on the development of the QE II storm. *Mon. Wea. Rev.*, **114**, 1019-1027.

-----, R. A. Petersen, K. F. Brill, P. J. Kocin, and J. J. Tuccillo, 1987: Synergistic interactions between an upper-level jet streak and diabatic processes that influence the development of a low-level jet and a secondary coastal cyclone. *Mon. Wea. Rev.*, **115**, 2227-2261.

Wallace, J. M., S. Tibaldi and A. J. Simmons, 1983: Reduction of systematic forecast errors in the ECMWF model through the introduction of an envelope orography. *Quart. J. Roy. Meteor. Soc.*, **35**, 455-463.

Wash, C. H., S. M. Heikkinen, C-S. E. Liou, and W. A. Nuss, 1990: A rapid cyclogenesis event during GALE IOP-9. *Mon. Wea. Rev.*, **118**, 375-391.

Whitaker, J. S., L. W. Uccellini, and K. F. Brill, 1988: A model-based diagnostic study of the rapid development phase of the Presidents' Day cyclone. *Mon. Wea. Rev.*, **116**, 2337-2365.

INITIAL DISTRIBUTION LIST

No. Copies

1.	Defense Technical Information Center Cameron Station Alexandria, VA 22304-6145	2
2.	Library, Code 0142 Naval Postgraduate School Monterey, CA 93943-5002	2
3.	Commander Naval Oceanographic Command Stennis Space Center, MS 39529-5000	1
4.	Commanding Officer Naval Oceanography Office Stennis Space Center, MS 39529-5001	1
5.	Commanding Officer Naval Oceanographic & Atmospheric Research Center Stennis Space Center, MS 39529-5004	1
6.	Commanding Officer Fleet Numerical Oceanography Center Monterey, CA 93943-5005	1
7.	Officer-in-Charge Naval Oceanographic & Atmospheric Research Center, Atmospheric Directorate Monterey, CA 93943-5006	1
8.	Director, Naval Oceanography Division Naval Observatory 34th and Massachusetts Avenue NW Washington, DC 20390	1
9.	Chairman, Oceanography Department U.S. Naval Academy Annapolis, MD 21402	1
10.	Chief of Naval Research 800 N. Quincy Street Arlington, VA 22217	1

11.   Prof. R. J. Renard, Code 63Rd   1
        Department of Meteorology
        Naval Postgraduate School
        Monterey, CA 93943-5000

12.   Prof. Carlyle H. Wash, Code 63Wx   8
        Department of Meteorology
        Naval Postgraduate School
        Monterey, CA 93943-5000

13.   Prof. Wendell A. Nuss, Code 63Nu   1
        Department of Meteorology
        Naval Postgraduate School
        Monterey, CA 93943-5000

14.   Richard Hodur   1
        Naval Oceanographic & Atmospheric Research Center,
        Atmospheric Directorate
        Monterey, CA 93943-5006

15.   Chi-San Liou   1
        Naval Oceanographic & Atmospheric Research Center,
        Atmospheric Directorate
        Monterey, CA 93943-5006

16.   Rolf Langland   1
        Naval Oceanographic & Atmospheric Research Center,
        Atmospheric Directorate
        Monterey, CA 93943-5006

17.   Roland Picard   1
        Naval Oceanographic & Atmospheric Research Center
        Stennis Space Center, MS 39529-5004

18.   Ronald J. Miller   4
        Naval Oceanographic & Atmospheric Research Center,
        Atmospheric Directorate
        Monterey, CA 93943-5006